研究成果の刊行物・別刷り

Parasitology International 58 (2009) 36–44

Contents lists available at ScienceDirect

Parasitology International

journal homepage: www.elsevier.com/locate/parint

Proteome approach for identification of schistosomiasis japonica vaccine candidate antigen

Ekhlas Hamed Abdel-Hafeez [a], Mihoko Kikuchi [a,b], Kanji Watanabe [c], Takashi Ito [d,e], Chuanxin Yu [f], Honggen Chen [g], Takeshi Nara [h], Takeshi Arakawa [i], Yoshiki Aoki [c], Kenji Hirayama [a,e,*]

[a] Department of Immunogenetics, Institute of Tropical Medicine (NEKKEN), Nagasaki University, 1-12-4 Sakamoto, Nagasaki 852-8523, Japan
[b] Center for International Collaborative Research, Nagasaki University (CICORN), 1-12-4 Sakamoto, Nagasaki 852-8523, Japan
[c] Department of Parasitology, Institute of Tropical Medicine (NEKKEN), Nagasaki University, 1-12-4 Sakamoto, Nagasaki 852-8523, Japan
[d] Department of Biochemistry, Nagasaki University, School of Medicine 1-12-4 Sakamoto, Nagasaki 852-8523, Japan
[e] Global COE Program, Nagasaki University, 1-12-4 Sakamoto, Nagasaki 852-8523, Japan
[f] Jiangsu Institute of Parasitic Diseases, Meiyuan, Wuxi, Jiangsu 214064, PR China
[g] Jiangxi Provincial Institute of Parasitic Diseases, Nanchang 330046, PR China
[h] Department of Molecular and Cellular Parasitology, Department of Epidemiology and Environmental Health, Juntendo School of Medicine, Hongo 2-1-1, Bunkyo-ku,Tokyo 113-8421, Japan
[i] Division of Molecular Microbiology, Center of Molecular Biosciences, University of the Ryukyu, 1 Senbaru, Nishihara 903-0213, Okinawa, Japan

ARTICLE INFO

Article history:
Received 26 May 2008
Received in revised form 11 August 2008
Accepted 19 September 2008
Available online 7 October 2008

Keywords:
Schistosoma japonicum
Radiation-attenuated cercariae
Vaccine
Miniature pig
Proteome

ABSTRACT

Experimental vaccination with radiation-attenuated cercariae (RAC) confers possible practical levels of resistance to challenge infection by humoral and by cellular mechanism. Here, we aimed to identify possible vaccine antigens by using specific IgG antibody from RAC vaccinated miniature pig. Two milligrams of soluble egg antigen (SEA) or schistosomal worm antigen preparation (SWAP) was fractionated using two dimensional liquid chromatography (proteome PF 2D) consisted of high performance chromatofocusing (HPCF) and high resolution reversed phase chromatography (HPRP). Of the 42 HPCF fractions of SEA or SWAP, 26 (61.9%) or 15 (35.7%) showed positive dot blot reaction with RAC vaccinated serum respectively. The dot blot positive fractions were applied to the second HPRP column. One hundred and seven out of 26×96 of SEA fractions and 18 out of 15×96 SWAP fractions reacted with RAC vaccinated serum. From the positive fractions we chose 17 of SEA and 10 of SWAP that had no reactivity with normal cercariae infected (NCI) sera and had single peak of 214 nm; and automated N-terminal amino acid sequence based on in situ Edman Reaction was conducted. Four sequences were obtained and applied to the homology search in NCBI database. A total of eight candidate genes were listed up and their cDNA clones from schistosomula stage were obtained. Two of the recombinant proteins (AAW27472.1 and AXX25883.1) showed strong reactivity with the RAC vaccinated serum but marginal with NCI serum. This protocol using proteome PF 2D could be applicable in identifying immunoreactive proteins from crude extract for the development of vaccines or for diagnostics.

1. Introduction

Schistosomiasis is a parasitic disease which affects more than 200 million individuals in Africa, Asia and South America. It is endemic in 74 countries causing more than 250,000 deaths per year [1]. Despite two decades of comprehensive campaign for the control, the number of individuals with active schistosomiasis worldwide remains at about 200 million annually [2,3]. Vaccine has long been expected to be developed as a novel strategic tool for the control [4–6]. A comprehensive review on current status of vaccines for schistosomiasis had provided by McManus and Loukas [7].

There are three different approaches for isolation and identification of schistosome vaccine candidates [8,9]. Selection based on protective monoclonal antibodies such as glutathione-*S*-transferase (GST) [10] and triosephosphate isomerase (TPI) [11], by unique antigen recognition by strong natural resistance in humans [12] or animals [13], or by antigen selection using the radiation-attenuated cercariae vaccine (RAC) model [14–16]. For example, a fragment of myosin of *S. mansoni* (SmIrV-5); one of the vaccine candidate antigens selected by TDR/WHO committee [17], was identified using serum from mice exposed to RAC [18]. None of the antigens identified conferred equivalent efficacy of the vaccination using RAC [5,19,20]. There is a quantitative and/or qualitative difference between the immune responses generated by RAC vaccine and those by defined subunit vaccine [21,22]. Increased immunogenicity of

Abbreviation: RAC, radiated-attenuated cercariae; NCI, normal cercariae infected; NC, healthy control; SEA, soluble egg antigen; SWAP, schistosomal worm antigen preparation; HPCF, high performance chromatofocusing; HPRP, high resolution reversed phase chromatography.

* Corresponding author. Tel.: +81 95 819 7818; fax: +81 95 819 7821.
E-mail address: hiraken@nagasaki-u.ac.jp (K. Hirayama).

1383-5769/$ – see front matter © 2008 Elsevier Ireland Ltd. All rights reserved.
doi:10.1016/j.parint.2008.09.004

RAC is related to delayed and truncated pattern of migration, in contrast to the normal parasite [23]. In fact, radiation induces defects in the neuromuscular coordination of the developing larvae [24]. Accordingly, delayed parasite migration through skin or skin draining lymph nodes and lungs would mean that there is a greater opportunity for interaction of parasite antigen with the immune cells at these sites which may in turn favor the priming of the protective response.

The highest levels of resistance obtained in mice after vaccination with RAC require antibodies and T cells [25,26]. It is clear that protective immunity generated by RAC vaccines is mediated by acquired immune mechanisms that require the reactivation of antigen specific $CD4^+$ helper cells [27]. However, passive transfer experiments indicate that IgG antibodies are also the key mediators of this immunity [28–30].Thus, elucidation of antigens relevant to both humoral and cellular response may be critical for the development of an optimal vaccine.

Most of our knowledge on schistosomiasis is drawn from experiments in primates and rodents. Although primate model is relatively better but the high cost and ethical concerns make them difficult to be used [31]. Also the use of rodents has several problems as a model for schistosomiasis [32,33]. When we focus on RAC vaccine of *S. japonicum*, higher protection has been achieved in rhesus monkeys [34], in cattle [35,36] and in pigs [19]. Within the reservoir host animals, pig would be the easiest one compared with cattle or sheep, but still the major drawback of the domestic pig is the large body mass. For this reason we established a unique miniature pig model for human Schistosomiasis japonica [37]. In this study we aimed to identify the major antigenic molecules which are specifically recognized by RAC vaccinated serum of miniature pigs for identification of possible candidate schistosomiasis vaccine.

2. Materials and methods

2.1. Parasite

Chinese strain of *S. japonicum* was obtained from Jiangsu Provincial Institute of Parasitic Diseases Wuxi, Jiangsu Province, People's Republic of China. Cercariae were released from the infected snails by light induction as described [38]. Attenuation of the cercariae was carried out by 200 Gy of γ-irradiation at a rate of 33 Gy/min using ^{60}Co irradiator (Pony Industry CO. LTD. PS-3100sB, Osaka, Japan).

2.2. Preparation of cultured schistosomula

Cercariae were released from 100 infected snails in a beaker containing 200 ml of tap water under light for 2 to 3 h at room temperature and were passed through Sartorus Nylon spacer, mesh size 0.1 mm. The obtained suspension was centrifuged for 60 s at 1500 rpm (383 g) at 10 °C to concentrate cercariae. The cercariae were washed twice in Basal Medium Eagle (BME) (Gibco-Invitrogen Co., CA, USA) containing 15 mM of HEPES (Gibco-Invitrogen Co.), 300 units/l Penicillin (Gibco-Invitrogen Co.), 300 μg/l Streptomycin (Gibco-Invitrogen Co.) and 160 μg/l Gentamicin (Gibco-Invitrogen Co.) in aseptic condition. Transformation of cercariae to schistosomulae was carried out mechanically by shearing the tail using vortex for 3 min; and about 200–300 parasites/ml of the mechanically transformed shistosomulae were cultured in DMEM (Sigma-Aldrich Co., MO, USA) containing 1% Fetal calf serum (FCS) (Hyclone, UT, USA), 300 units/l penicillin and 300 μg/l streptomycin in 24 well plate (Corning, NY, USA) at 37 °C in 5% CO_2 incubator for 24 h. The cultured schistosomulae were collected by centrifugation, washed three times with phosphate buffered saline (PBS) and kept frozen at −80 °C until use [39].

2.3. Soluble worm antigen preparation (SWAP)

SWAP was obtained by the method described elsewhere [40]. Briefly, *S. japonicum* adult worms were obtained by perfusion of infected rabbits. After lyophilization, worms were homogenized in cold diethyl ether and centrifuged to remove lipids. The pellet was then freeze–thawed several times in PBS, pH 7.4 containing 1 mM phenyl methyl-sulphonyl fluoride (PMSF) and 2 μg/ml Leupeptin (Sigma). The homogenate was dialyzed against several changes of PBS at 4 °C, and centrifuged at 30,000 g for 50 min at 4 °C. The supernatant was filtrated through 0.22 μm filter (Millipore Co., MA, USA) and this was used as SWAP. Protein concentration was determined by BCA protein Assay Kit (Pierce Biotechnology, Inc., IL, USA).

2.4. Soluble egg antigen preparation (SEA)

Preparation of SEA was previously described [41]. Briefly, *S. japonicum* eggs were isolated from infected liver and intestine of rabbit. The purified eggs were finally adjusted to a concentration of 50,000 eggs/ml of PBS with 1 mM of PMSF, and 2 μg/ml Leupeptin (Sigma) and sonicated three times on ice for 10 min. The suspension was freeze–thawed several times and centrifuged at 30,000 g for 50 min at 4 °C. The supernatant was filtrated through 0.22 μm filter; and this was used as SEA. Protein concentration was determined by BCA protein assay.

2.5. Experimental animals, parasitological examinations and serum sample collection

Six-week-old male CLAWN strain miniature pigs (Japan farm, Kagoshima, Japan) weighing between 2.5 kg and 3 kg were used in this study. The pigs were fed with standard feed based on their body weights, with water ad libitum. Seven pigs were used, three for immunization with radiation-attenuated cercariae (RAC) of *S. japonicum*, three for infection with 200 cercariae (NCI) and one as a healthy control (NC). Sera were collected four weeks after vaccination and four weeks after challenge by drawing blood from auricular vein at indicated times. Before taking blood, pigs were anesthetized by intramuscular injection with 0.2 mg/kg midazolam (Yamanouchi Pharmaceutical Co., Ltd. Tokyo, Japan) and 40 μg/kg medetomidine (Orion Corp., Espoo, Finland). The first group of pigs was subjected to a single percutaneous exposure of 400 RAC using a cover slip as described [37]. Four weeks later, the first and second groups of pigs were challenged with 200 normal cercariae (NCI). The third group was used as a healthy control. Feces were collected every week and the number of eggs excreted into feces was counted as previously described [37]. Adult worms were recovered from the liver and mesenteric veins as described [20]. The experimental protocol was approved by the Animal Ethical Committee of Nagasaki University (No.0204250127-3).

2.6. SDS-PAGE and western blot analysis

SWAP and SEA were boiled for 5 min in reducing sample buffer containing 4% sodium dodecyl sulfate (SDS) and 50 mM Dithiothreitol (DTT), and electrophoresed by using 5–20% gradient SDS polyacrylamide gel (E-pagel®, Atto Co., Tokyo, Japan) [42]. For the western blot analysis, SEA and SWAP proteins separated by the E-pagel were transferred onto PVDF membrane (Millipore Co.). After blocking in 5% skimmed milk in Tris-buffer (TBS-Tween 20) (20 mM Tris–HCl, pH 7.5; 500 mM NaCl; 0.1% Tween 20) for 1 h at room temperature, the protein transferred-membrane was incubated with the 3000 times diluted test serum for 2 h at room temperature. After washing three times with TBS-Tween 20, the membrane was incubated in 10 ml of a secondary antibody solution containing 40,000 times diluted affinity Purified anti-porcine IgG antibody that is horseradish peroxidase

Table 1
Fecal egg excretion of RAC immunized and none immunized miniature pigs after challenge infection with 200 cercariae of *S. japonicum* Chinese strain

Examination time after challenge infection	EPG (egg per gram of feces)		P[c]
	RA[a] (n=3)	NC[b] (n=3)	
5th week	74.34±82.26	102.81±81.47	NS
(EPG of individual)	(190.65, 18.65, 13.71)	(45.03, 196.00, 67.4)	
6th week	265.03±151.25	413.42±171.92	0.028
(EPG of individual)	(438.78, 193.48, 162.82)]	(610.00, 291.13, 339.14)	
7th week	180.68±104.29	389.85±254.99	NS
(EPG of individual)	(298.61, 142.86, 100.57)	(681.03, 206.42, 282.10)	
8th week	156.24±99.28	558.26±181.23	0.026
(EPG of individual)	(265.91, 130.36,72.46)	(686.22, 637.68, 350.88)	
9th week	207.42±79.60	480.61±76.57	0.003
(EPG of individual)	(280.49, 219.18, 122.95)	(528.69, 520.83, 392.31)	

The values in parentheses represent the EPG for each pig.
[a] RA: vaccinated with 400 RAC.
[b] NC: no vaccination control.
[c] *P* values were calculated by two tailed Student's *t*-test.

(HRP) conjugated (Anti pig IgG (H+L)-HRP, AP166P, Chemicon International, CA, USA) and TBS-Tween 20 for 1 h at room temperature. After washing three times with TBS-Tween 20, reactive protein bands were visualized by exposing an x-ray film using ECL-Plus Western blotting Detection system (G. E. Healthcare, Amersham Biosciences, Buckinghamshire, UK).

2.7. Protein purification and fractionation

The protein purification and fractionation of SWAP and SEA were performed using Proteome Lab PF 2D system (Beckman Coulter, CA, USA) that is designed for two dimensional liquid chromatography consisted of a high-performance chromatofocusing (HPCF) in the first dimension followed by high-resolution reversed-phase chromatography (HPRP) in the second dimension. One milliliter of 2 mg/ml of either SWAP or SEA was introduced with a manual injector into the column for the first dimensional HPCF. The protein was bound to a strong anion exchanger followed by elution with a continuously decreasing pH (8.5–4.0) gradient (Beckman Coulter). The proteins were eluted based on their isoelectric point (pI), collected in a 96 deep-well plate (Beckman Coulter) [43]. The first dimensional fractions were directly applied to the second HPRP in a C18 column. The mobile phase consisted of two buffers, the first one 0.1% Trifluoroacetic acid (TFA) in water and the second one 0.08% TFA in acetonitrile. Separation was performed according to the Manufacturer's instruction protocol.

2.8. Dot blot ELISA

The fractions were blotted onto a PVDF membrane (Millipore Co.) using the Bio-Dot ® SF Micro filtration apparatus (Bio Rad Laboratories, Inc., CA, USA). Briefly, 20 µl of each fraction were blotted onto the PVDF membrane and the membrane was soaked in 5% skimmed milk in Tris-buffer (TBS-Tween 20) for 1 h at room temperature. The membrane was incubated with 1000 times diluted test serum for 2 h at room temperature. The reactivity of each dot with test serum was estimated by the dot blot ELISA using the same method described above in the western blotting. We selected positive dots when they showed increased intensity compared with those incubated with normal control serum. The criteria that used for selection of the positive/negative results of dot-ELISA are using two positive controls, the crude antigens of SWAP and SEA, and PBS as a negative control. All the positive fractions of the first dimension were sequentially applied to the second dimensional HPRP.

2.9. Amino acid sequencing

Fractions from the second dimensional HPRP were analyzed by dot blot ELISA and positive fraction was subjected to amino acid sequencing. Two hundred microliters of positive fraction was spotted onto Polybrene-coated glass fiber discs. Subsequently proteins were sequenced with an automated protein sequencer (ABI Model cLc; Applied Biosystem, CA, USA).

Table 2
Worm numbers recovered from each group of miniature pigs

Pig group	Worm burden			
	Total	Male	Female	Reduction rate[b]
RA 1	5	4	1	96.4%
RA 2	42	36	6	69.7%
RA 3	51	44	7	63.2%
Average	32.67	28.0	4.67	76.4%
NC 1	160	135	25	-
NC 2	117	87	30	-
NC 3[a]	-	-	-	-
Average	138.5	111.0	27.5	-

NC3[a]: this pig died at the 9th week after infection due to sudden death.
Reduction rate [b]: The worm reduction rate=(the average worm burden in the control group−the worm burden in the vaccinated group)/(the average worm burden in the control group)×100.

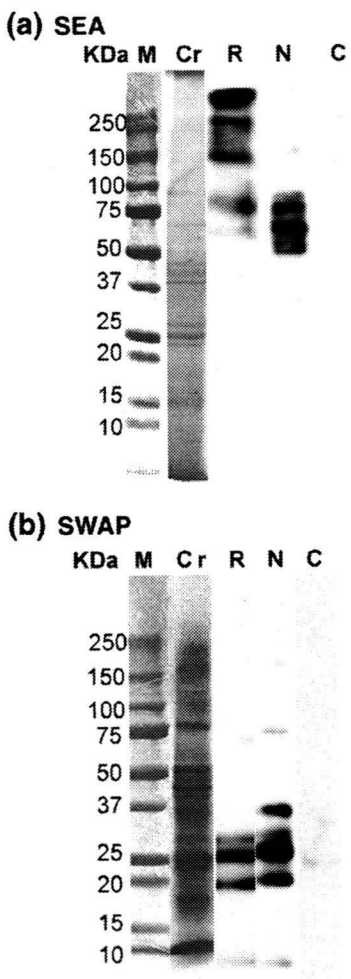

Fig. 1. SDS-PAGE and western blot analysis of RAC (R), NCI (N) and NC (C) sera of miniature pig for the specific IgG against (a) SEA and (b) SWAP. Lane M: molecular weight marker; lane Cr: CBB staining of the crude extract; lanes R, N and C: Western blot pattern probed with a panel of sera; lane R: RAC serum; lane: N. NCI serum and lane: C NC serum. Sera were diluted 3000 times.

2.10. Homology search

The obtained amino-terminal sequences were blast-searched for their homology with the genes deposited in the *S. japonicum* database in NCBI using BLAST/blastp suite programs, in non redundant Gene Bank Coding Sequence (CDS). After homologous genes were listed up, further selection was performed according to the following criteria; the homologous area should be located at the N-terminus sequences and its deduced pH must be within the pI range of first dimensional fraction.

2.11. mRNA analysis

To confirm mRNA expression of the candidate genes in the different stages of the parasites, total RNA was extracted from cercariae, 24 h cultured schistosomulae, eggs, and adult worms of *S. japonicum* according to the instruction manual of Micro-to-midi total RNA purification system kit (Invitrogen Co.). The first strand cDNA was synthesized from the total RNA by using oligo (dT) primer according to the instruction manual of high capacity cDNA reverse transcription Kit (Applied Bio systems) and was used as template for reverse transcript PCR using a set of primers that were designed from the candidate gene as indicated in the Table 4. *S. japonicum* actin gene primers were used as an internal reference. RT-PCR was performed by the following condition of 42 cycles of 30 s at 94 °C, 50 s at 55 °C and 2 min at 72 °C for all samples. PCR products were subsequently separated on 1% agarose gel, stained with ethidium bromide and visualized under UV light. The resulting PCR products were cloned into pCR 2.1 using TOPO-TA cloning Kit (Invitrogen Co.), sequenced using Big-Dye V.1.1 terminator cycle sequencing Kit (Applied Biosystem) and analyzed on an ABI 3710 DNA Sequencer (Applied Biosystem) for confirmation with database sequences.

2.12. Production of recombinant protein

Reverse-PCR products from cercarial mRNA purified from agarose gel were cloned into the pET/100 D-TOPO expression vector (Invitrogen Co.) and transformed into chemically competent TOP10 *Escherichia coli* (Invitrogen Co.) according to the manufacturer's protocol. Cells were plated onto LB-Ampicillin (50 μg/ml) plates and incubated for 18 h at 37 °C. Ten positive clones were identified and were grown for 18 h in 6 ml LB medium containing Ampicillin (50 μg/ml) and plasmids prepared using a Gene Elut™ plasmid Miniprep kit (Sigma). Plasmids were then digested with Nhe I and Sac I (New England Biolabs, MA,USA) for 2 h at 37 °C and the inserts detected by separating the DNA on a 1% agarose gel stained with ethidium bromide and visualized under U.V. light.

To confirm the correct orientation and in frame, the inserts were sequenced using Big-Dye V.1.1 terminator cycle sequencing Kit (Applied Biosystem) and analyzed on an ABI 3710 DNA Sequencer (Applied Biosystem). Plasmid DNA containing expression constructs was transformed into BL21 Star™ (DE3) One Shot® *E. coli* (Invitrogen Co.) for recombinant protein expression. Briefly, 10 ng of plasmid DNA was transformed into the bacteria by heat shocking at 42 °C for 30 s. Transformed bacteria were grown overnight at 37 °C in LB medium supplemented with either 100 μg/ml ampicillin or 50 μg/ml

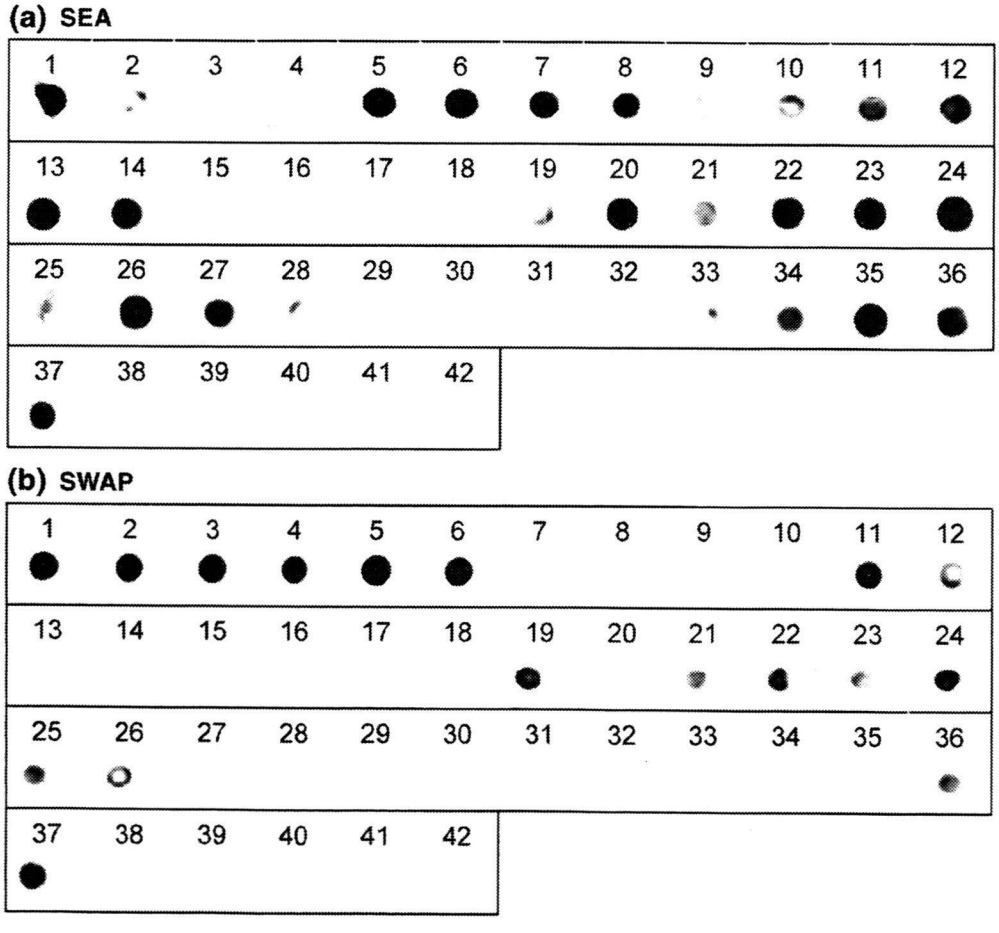

Fig. 2. Dot blot analysis of (a) SEA and (b) SWAP fractions of HPCF using pooled RAC vaccinated sera were diluted 1000 times. Dot blot has been repeated twice and the representable positive fractions to RAC serum were selected.

Table 3
Dot blot analysis of the first and second fractions of SEA and SWAP that reacted with RAC vaccinated and/or NCI serum from miniature pigs

Sequential screening steps		No. of the RAC positive fractions (%)	
		SEA (%)	SWAP (%)
1st dimension	(42 Frs. of SEA, 42 Frs. of SWA)	26 (61.9)	15 (35.7)
2nd dimension	(2496 Frs. of SEA, 1440 Frs. of SWA)	107 (4.3)	18 (1.3)
NCI (−)	(107 Frs. of SEA, 18 Frs. of SWA)	61 (57)	10 (55)
Single peak (+)	(61 Frs. of SEA, 10 Frs. of SWA)	17 (27.87)	10 (100)

Frs.: Fractions.
NCI (−): Dot blot fractions that did not react with Normal Cercaria Infection serum.
Single peak (+): Dot blot fractions that have single retention peak were selected to amino acid sequencing.

carbenicillin prior to pilot expression by the addition of Isopropyl β-D-1-thiogalactopyranoside (IPTG) as an inducer according to the manufacturer's protocol (Invitrogen Co.). Briefly, 10 ml of LB medium containing 100 μg/ml ampicillin or 50 μg/ml carbenicillin was inoculated with 500 μl of an overnight culture and allowed to grow for 2 h at 37 °C with shaking until they reached mid-log phase of growth. IPTG was then added to a final concentration of 0.1 mM to 0.5 mM and a 500 μl aliquot was removed from the culture, centrifuged at 10,000 g in a micro centrifuge for 30 s. The supernatants were removed and the cell pellets frozen at −20 °C. Remaining cultures were incubated at 37 °C with shaking and 500 μl aliquots were removed after 1, 2, 4 and 6 h post-induction. Individual sample was analyzed by SDS-PAGE and western blot for detection of recombinant protein using Anti-His G-HRP Antibody (Invitrogen Co.).

3. Results

3.1. Protective response in miniature pig vaccinated with radiation-attenuated cercariae (RAC)

The mean of fecal egg excretion of RAC vaccinated group was significantly reduced at 6th, 8th and 9th weeks post infection, when compared to the control group as shown in Table 1. The recovered worm number after the perfusion also indicated the vaccination effect of RAC as shown in Table 2.

3.2. Antigen recognition by sera from the vaccinated miniature pigs

We aimed to identify the antigenic molecules reactive with RAC vaccinated serum of miniature pigs but not with serum from those just infected with 200 cercariae for 4 weeks. As a target antigen preparation, we used SEA and SWAP antigens [16].

Pooled sera obtained 4 weeks after the RAC vaccination recognized antigenic molecules of 263, 255, 155, 130, 78, 55 and 20 kDa from SEA as shown in lane (R) of Fig. 1a. Whereas sera obtained 4 weeks post challenge with 200 normal cercariae, recognized antigens of 253, 155, 130, 74, 60, and 37.5 kDa (lane N of Fig. 1a). When we used SWAP, pooled sera obtained 4 weeks after the RAC vaccination recognized antigens of 70, 27, 21 and 10 kDa as shown in lane R of Fig. 1b. Sera obtained 4 weeks post challenge with normal cercariae recognized antigens of 150, 71, 36, 27, 21 and 10 kDa (lane N, Fig. 1b). The pooled sera used in this experiment were diluted 3000 times.

3.3. First dimension: high-performance chromatofocusing (HPCF)

Following the HPCF fractionation of SEA and SWAP 42 fractions were obtained. All the 42 fractions from SEA or SWAP were tested for reactivity with RAC vaccinated pooled serum as shown in Fig. 2a and b. Totally 26 SEA and 15 SWAP fractions were reacted to RAC vaccinated pooled serum as shown in Table 3.

3.4. Second-dimension: high performance reversed-phase chromatography (HPRC)

Those 26 and 15 dot blot positive fractions of SEA and SWAP respectively, from the first dimension (HPCF) were subjected to further fractionation by the HPRC. The Proteome maps of the second dimensional separation are shown in Fig. 3a and b.

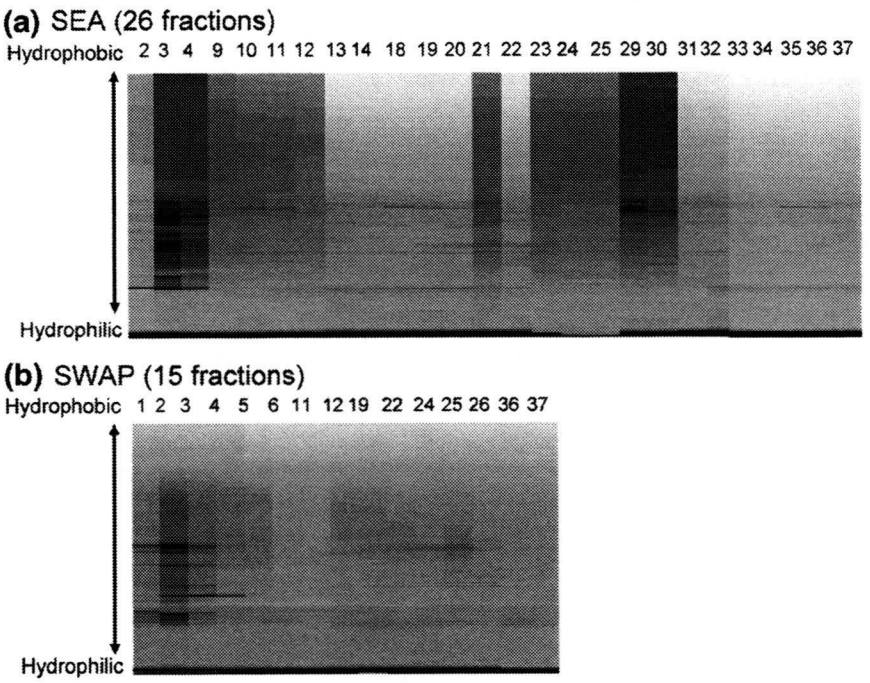

Fig. 3. The Proteo Vue ® MAP of the second dimensional separation for the positive dot blot fractions from SEA (a) and SWAP (b). Hydrophobicity of each fraction is expressed by its retention time. Each band represents Optical Density of a peptide at 214 nm. The fraction numbers of the first column are shown on top of the figures.

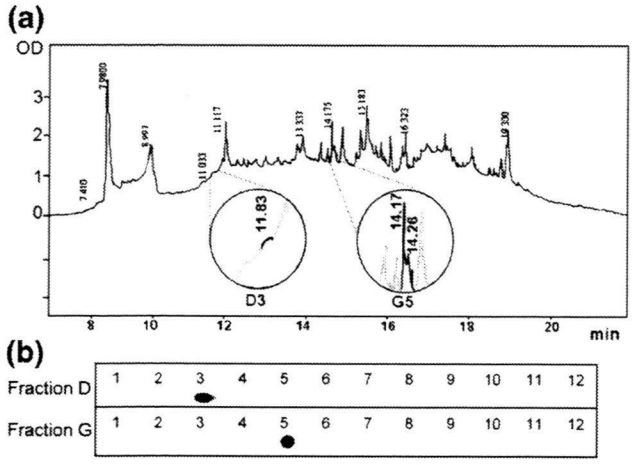

Fig. 4. Representative of the second column separation of the first fractions (fraction No.2 of SEA) (a) and the dot blots analysis for the fraction No. 2 of SEA (b). (a) The optical densitometry pattern (OD at 214 nm) is represented. The x axis represents retention time in min according to the concentration of acetonitrile in the mobile phase. (b) D3 and G5 are the two fractions obtained from the 96-well plate that was used for collection of the second column separation.

Elution pattern of the fraction number 2 of SEA after the second column is shown in Fig. 4a, as an example. All the fractions obtained after the second column were tested for reactivity against the RAC vaccinated serum. Out of the 2496 SEA and 1440 SWAP fractions, 107 and 18 fractions reacted with the RAC vaccinated serum respectively, as shown in Table 3. These 107 and 18 positive fractions were further tested for reactivity with normal cercariae infected (NCI) serum. Out of the 107 SEA and 18 SWAP fractions, 46 and 8 fractions reacted with NCI serum respectively (Table 3). Dot blot pattern for fraction number 2 of SEA after second column separation was shown in Fig. 4b as an example. D3 and G5 fractions showed strong reactivity and D3 fraction had single retention peak while G5 fraction had two peaks as shown in Fig. 4a. The pooled sera used in dot blotting experiments were diluted 1000 times.

3.5. Amino acid sequencing

As shown in Table 3, after identification of 107 SEA and 18 SWAP fractions, we selected 61 SEA and 10 SWAP fractions by excluding the fractions reactive to NCI serum. For amino acid sequencing, we analyzed their retention peak patterns as shown in Fig. 4a, and picked 17 from SEA and 10 from SWAP that had single peak. Finally we obtained four N-terminal sequences, 2 from SEA and 2 from SWAP as shown in Table 4.

3.6. Homology search

The four identified N-terminal amino acid sequences were applied to the NCBI/BLAST/blastp suite programs. After the homology search we set the selection criteria of the candidate genes as follows, (1) high homology on the N-terminal sequences (2) deduced pH compatible with the pI range of first dimension. Two candidate genes for each amino acid sequence were selected as shown in Table 4.

Table 4
The amino acid sequences obtained from the fractions and the candidate genes with their homology and pI range

Fraction no.	pH range	N-terminal seq.	Identified homology	Accession no.	pI[a]
F29.2E. SEA	pH<4.80	MCVLPVD	60 CILPVD 65	AAX24607.2	4.70
			39 CVLP–43	AAW27155	4.60
F2.3D.SEA	8.49–8.4	MAVLPPIYKYL	3———PILYKYL 9	AAW27472.1	8.03
			281 MAVLP——— 285	AAW26143.1	8.02
F12.H1. SWAP	8.40–8.10	VPTNQN	415-PTNQ-418	AAW27566	8.39
			211-PTSQN 215	AAW26607.1	8.40
F12.F1. SWAP	8.40–8.10	KRRGPPGEER	131-RRSNPPTEE-139	AAW27690.1	8.49
			19———PPSEE-23	AAX25883.1	8.49

[a] pI: has been calculated from DNAstar software (DNASTAR Inc., Madison, WI, USA).

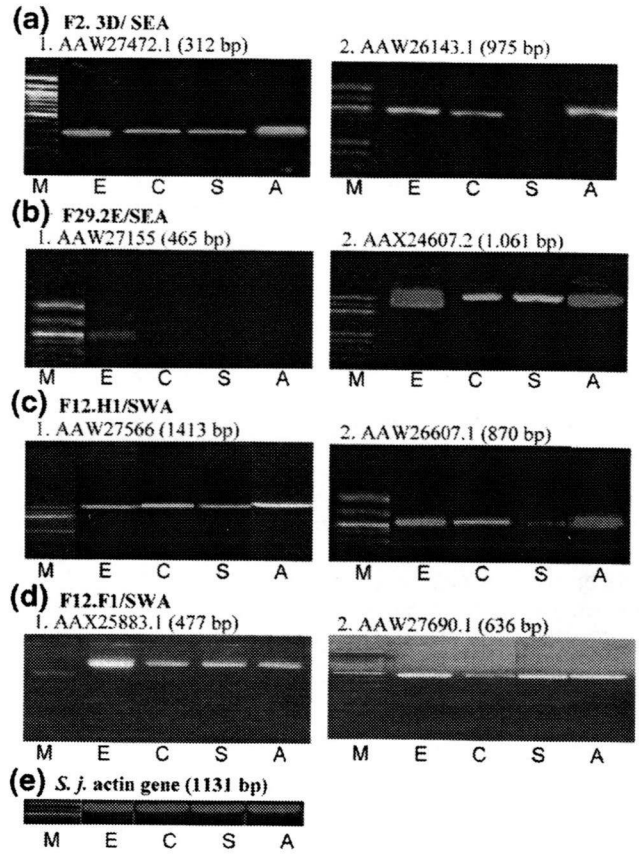

Fig. 5. mRNA expression of the selected candidate genes from different developmental stages of *S. japonicum*. PCR fragments with expected size amplified from the different stages of the *S. japonicum* were obtained using primer sets designed for the eight candidate genes and the actin gene as a control. Lane M: molecular weight maker; lane E: egg; lane C: cercariae; lane S: 24 h cultured schistosomula; lane A: adult worm. (e) *Schistosoma japonicum* actin gene.

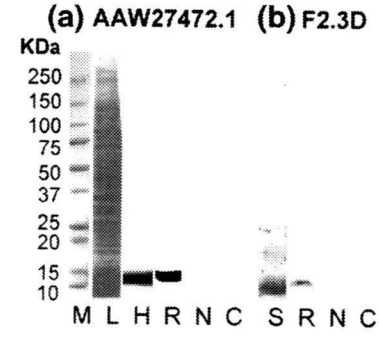

Fig. 6. Reactivity of the recombinant protein of AAW27472.1 (a) and its original fraction, F2.3D/SEA (b) with RAC vaccinated serum. (a) Lane M: molecular weight marker; lane L: CBB stained pattern of total lysate after induction with IPTG. Lanes H, R, N and C Western blotting patterns of the total lysate probed with a panel of sera; lane H: Anti histidine tag antibody; lane R: RAC serum; lane N: NCI serum; lane C: NC serum. (b) Lane S: Silver staining patterns of the original fraction, F2. 3D fraction. Lanes R, N and C: Western blotting patterns of the F2. 3D fraction probed with a panel of sera; lane R: RAC serum; lane N: NCI serum and lane C: NC serum.

3.7. Expression of mRNA encoding the candidate genes in different developmental stages

mRNA from eggs, cercariae, 24 h culture schistosomulae and adult worms of the Chinese strain of *S. japonicum* was used for RT-PCR amplification of the selected candidate genes. All the candidate genes were expressed in all the stages of the parasite, as shown in Fig. 5, except for the genes AAW27155 that was expressed only in the egg stage and AAW26143.1 that is expressed in the egg, cercariae and adult but not in schistosomulae (Fig. 5). All the amplified PCR fragments had exactly the expected molecular weight as in the NCBI database.

3.8. Recombinant and native protein reactivity with RAC vaccinated serum

Protein expression in *E coli* using recombinant pET100/D-TOPO expression vector bearing each PCR fragment was confirmed by the detection of a band in Coomassie Brilliant blue stained SDS-PAGE after IPTG induction and by western blotting probed with Anti His-tag Antibody or with vaccinated sera (data not shown). Two candidate genes named AAW27472.1 (Fig. 6) and AAX25883.1 (Fig. 7) with recombinant proteins having molecular weights 15.5 kDa and 24 kDa respectively were strongly recognized by RAC vaccinated sera but not reactive with NCI or NC sera. While the recombinant protein AAW27690.1 whose molecular weight was 35 kDa showed weak reactivity with RAC vaccinated serum but strong reactivity with NCI as shown in Fig. 7. Original native protein fractions of AAW27472.1, AAX25883.1 and AAW27690.1 that were F2.3D for AAW27472.1 and F12.1F for the latter two genes were analyzed by the western blotting analysis to compare with the recombinant protein patterns. As is shown in Fig. 6, native protein that corresponds to the same molecular weight around 11 kDa of the recombinant was detected by RAC serum.

Fig. 7 also shows strong reactive band of around 18 kDa in the F12.1F native fraction with RAC serum but not with NCI serum that may correspond to the AAX25883.1 recombinant protein of 21 kDa. Interestingly F12.1F fraction contained reactive band of 25 kDa with NCI serum that almost correspond to AAW27690.1 recombinant pattern.

4. Discussion

We have already reported that high levels of protective immunity were obtained by UV-attenuated cercaria vaccination in Chinese domestic pigs [20]. In this study we used CLAWN miniature pigs for vaccination with RAC and observed a comparable level of protective immunity as seen in the domestic pigs (Table1). Previous studies have shown that serum of RAC vaccinated mice can transfer protective immunity to naive recipients [25,44]. We concentrated on the analysis of antibodies in the development of resistance in this RAC vaccine miniature pig model.

In the present study, sera from RAC vaccinated pigs reacted with a number of proteins of SEA whereas sera collected from NCI showed different pattern of reaction (Fig. 1a).

The strong reactivity to SEA by the RAC vaccinated and NCI pigs could be explained by cross-reactivity of the provoked antibodies against components of cercaria to schistosomula stage worms or by the existence of common molecules shared between young worm and eggs. The significant difference of the reactive SEA proteins against RAC vaccinated and NCI sera suggests that the mode of immunization is different between those two methods [45,46].

It is well known that much of the antibodies of infected subjects are directed against carbohydrate determinants from the adult worms and the eggs [47]. We confirmed our major RAC vaccinated antibodies were directed against peptide by treating crude SEA and SWAP with glycopeptidase A, to remove the glycoconjugates. This treatment did not abolish the basic reactivity detected by the western blotting patterns of SEA or SWAP (data not shown).

Then we tried to identify a series of unique proteins that are recognized by RAC vaccinated sera but not by normal cercaria infected sera (NCI). As shown in Fig. 2 and Table 3, two-dimensional (2D) liquid chromatography successfully resolved the peptides that were shown to be reactive to RAC vaccinated serum. Although it is not clear that the 2D-LC has significant advantage over the 2D-SDS PAGE, using 2nd dimensional column, we could physically separate totally 2496 SEA fractions from 42 positive fractions of the first dimensional column and identified 107 fractions that were specifically reactive with RAC serum. Separation of intact proteins coupled with fraction collection was another advantage for this method [43]. Although our Edman degradation method could not identify many peptides, the discrimination ability from such a crude extract can be tolerated for further study.

We successfully obtained enough length of N-terminal sequences; 4 fractions out of 27 (Table 4). As shown in Figs. 6 and 7, even after the 2D column separation, each fraction contained several proteins as visualized by silver staining or by western blotting. The overall efficiency of the N-terminal sequencing of the fractions by the Edman Reaction is dependant on the purity and quantity so that we might have picked up major peptide's sequences in terms of quantity. Of course there is a fact that many schistosomal proteins were glycosylated and were possibly N-terminally blocked for the Edman Reaction. There is no doubt that MS-based protein identification is much faster and technically easier and currently the first choice over Edman degradation. Despite the fact that most of biological samples are a mixture even after physical separation as used in this study, the power of MS-based protein identification currently available should enable estimation of likeliness and relative abundance of identified proteins based on the number of peptides and coverage. The MS-based method must be more promising for this kind of identification.

After we got four sequences, the current database of ESTs from *S. japonicum* was used for the homology search. Unexpectedly, we have got only a limited level of homology to all the input sequences as was also noticed in the previous study [48]. Because of a large size of *S. japonicum* genome, it has not been subjected to full scale genome sequencing; [49,50]. Of course ESTs do not cover full length of the coding regions and a limited portion of transcripts are likely deposited in the EST database [51]. In order to increase the probability of selection of the candidate genes that were picked by their homology, pI was set as a second criterion for the selection (Table 4). His-tag fused recombinant proteins from the entire listed candidate genes were confirmed by western blotting using anti-his tag antibody and by

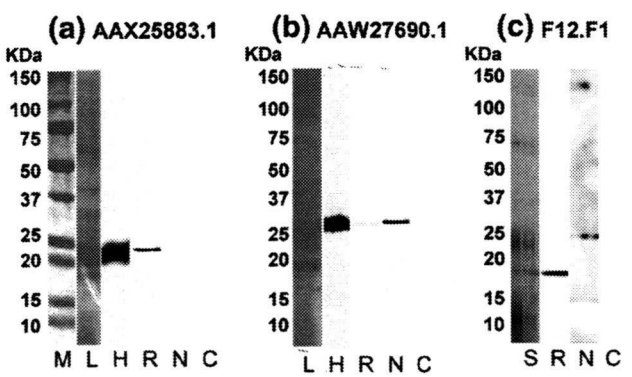

Fig. 7. Reactivity with RAC vaccinated serum of the recombinant proteins of AAX25883.1 (a) and AAW27690.1 (b) and that original fraction, F12.1F SWAP (c). (a) and (b) Lane M: molecular weight marker; lanes L: CBB stained pattern of total lysate after induction with IPTG. Lanes H, R, N and C: Western blot patterns of the total lysate probed with a panel of sera; lanes H: Anti histidine tag antibody lanes R: RAC serum; lanes N: NCI serum and Lanes C: NC serum. (c) Lane S: Silver staining patterns of the original fraction F12. F1 fraction). Lanes R, N and C: Western blotting patterns of the F12. F1 fraction probed with a panel of sera; lane R: RAC serum; lane N: NCI serum and lane C: NC serum.

their expected molecular weights, and only three recombinant proteins of AAW27472.1, AAX25883.1 and AAW27690.1 showed reactivity to RAC vaccinated serum.

The recombinant proteins obtained from the cloned AAW 27472.1 and AX25883.1 were highly reactive to RAC vaccinated serum but marginal with NCI serum that exactly reproduced the original fraction's behavior (Figs. 6 and 7). While the recombinant protein obtained from the cloned AAW27690.1 showed weak reactivity with RAC vaccinated serum, it showed strong reactivity with NCI as shown in Fig. 7. Therefore, AX25883.1 is more probable to match with the obtained N-terminal sequence.

The expected molecular weight of AAW27472.1 was 12.475 kDa but the protein in original purified fraction showed about 11 kDa as shown in Fig. 6. This may be a result of post-translation modification that often occurs in schistosomes [52]. AAW27472.1 was revealed to be a hypothetical protein, but had 23% homology with Cathepsin B endopeptidase (*S. japonicum*), and had 26% homology with cathepsin B endopeptidase (*S. mansoni*). In contrast to AAW27472.1, the expected molecular weight of AAX25883.1 was 18 kDa, and the protein in original purified fraction showed same molecular weight as shown in Fig. 7. AAX25883.1 was revealed to be a Syntaxin N-terminus domain that is a neuron system-specific protein implicated in the docking of synaptic vesicles with the presynaptic plasma membrane and had 23% homology with crystal structure of the 26 kDa glutathione S-transeferase of S. *japonicum*. The expected molecular weight of AAW27690.1 was 25 kDa, and the protein in original purified fraction, showed the same molecular weight as expected as shown in Fig. 7. AAW27690.1 was revealed to be a NADH ubiquinone oxidoreductase subunit of NDUFA12 and had 26% homology with "NADH dehydrogenase subunit 5". As the original purified fraction showed a reactive band around 25 kDa, this may be explained by the same reason as AAW27472.1.

In the present study, we have focused on the identification of soluble proteins and did not analyse the membrane protein that is expected to be another source of vaccine candidates. This 2D column system is applicable to the detergent solubilized membrane proteins using 2% Trion X-100 [53]. Membrane protein must be the next target for our study.

Although we have not yet examined the efficacies of these subunit candidate vaccines, we concluded that our 2D column protein fractionation system was simple and effective to identify the immuno-reactive proteins from crude extract.

Acknowledgements

This study was supported in part by the Grant-in-Aid for 21c COE program, Nagasaki University (2005–2010) and Grant-in-Aid for Exploratory Research (19659106) from the Ministry of Education, Culture, Sports, Science and Technology (MEXT), Health and Labour Sciences Research Grants (Research on Emerging and Re-emerging Infectious Diseases, H18-Shinko-Ippan-008) and Health and Labour Sciences Research Grants (Research on International Cooperation for caring Societies, H19-Kokui-Shitei-004) from the Ministry of Health, Labour and Welfare of Japan. And grant from US-Japan-Cooperative Medical Science Program (Parasitic Disease). E. H. A. is a recipient of the Egyptian government scholarship.

References

[1] Van der Werf MJ, De Vlas SJ, Brooker S, Looman CW, Nagelkerke NJ, Habbema JD, et al. Quantification of clinical morbidity associated with schistosome infection in sub-Saharan Africa. Acta Trop 2003;86:125–39.
[2] Bergquist NR. Schistosomiasis vaccine development: progress and prospects. Mem Inst Oswaldo Cruz 1998;93:95–101.
[3] Ross AG, Bartley PB, Sleigh AC, Olds GR, Li Y, Williams GM, et al. Schistsomaiasis. N Engl J Med 2002;346:1212–20.
[4] McManus DP. The search for a vaccine against schistosomiasis – a difficult path but an achievable goal. Immuno-Rev 1999;171:149–61.
[5] McManus DP, Bartley PB. A vaccine against Asian schistosomiasis. Parasitol Int 2004;53:163–73.
[6] Bergquist NR, Leonardo LR, Mitchell GF. Vaccine-linked chemotherapy: can schistosomiasis control benefit from an integrated approach? Trends Parasitol 2005;21:112–7.
[7] McManus DP, Loukas A. Current status of vaccines for schistosomiasis. Clin Microbiol Rev 2008;21:225–42.
[8] McManus DP. Prospects for development of a transmission blocking vaccine against *Schistosoma japonicum*. Parasite Immunol 2005;27:297–308.
[9] Wu ZD, Lü ZY, Yu XB. Development of a vaccine against *Schistosoma japonicum* in China: a review. Acta Trop 2005;96:106–16.
[10] Xu CB, Verwaerde C, Grzych J-M, Fontaine J, Capron A. A monoclonal antibody blocking the *Schistosoma mansoni* 28-kDa glutathione S transferase activity reduces female worm fecundity and egg viability. Eur J Immunol 1991;21:1801–7.
[11] Harn DA, Gu W, Oligino LD, Mitsuyama M, Gebremichael A, Richter DA. Protective monoclonal antibody specifically recognizes and alters the catalytic activity of schistosome triose-phosphate isomerase. J Immunol 1992;148:562–7.
[12] Acosta LP, Aligui GD, Tiu WU, McManus DP, Olveda RM. Immune correlate study on human *Schistosoma japonicum* in a well-defined population in Leyte, Philippines: I. Assessment of resistance versus susceptibility to *S. japonicum* infection. Acta Trop 2002;84:127–36.
[13] Techau ME, Johansen MV, Lind P, Ornbjerg N. The effect of colostrum on pigs prenatally or postnatally exposed to *Schistosoma japonicum*. Parasitology 2004;129:597–604.
[14] Hooker CW, Brindley PJ. Cloning of a cDNA encoding SjIrV1, a *Schistosoma japonicum* calcium-binding protein similar to calnexin, and expression of the recombinant protein in *Escherichia coli*. Biochim Biophys Acta 1999;1429:331–41.
[15] Zhang Y, Taylor MG, McCrossan MV, Bickle QD. Molecular cloning and characterization of a novel *Schistosoma japonicum* irradiated vaccine-specific antigen, Sj14-3-3. Mol Biochem Parasitol 1999;103:25–34.
[16] Richter D, Harn DA. Candidate vaccine antigens identified by antibodies from mice vaccinated with 15- or 50-kilorad-irradiated cercariae of *Schistsoma mansoni*. Infect Immun 1993;61:146–54.
[17] Bergquist NR, Colley DG. Schistosomiasis vaccines: research to development. Parasitol Today 1998;14:99–104.
[18] Dalton JP, Tom DT, Strand M. Cloning of a cDNA encoding a surface antigen of *Schistosoma mansoni* schistosomula recognized by sera of vaccinated mice. Proc Natl Acad Sci 1987;84:4268–72.
[19] Shi YE, Jiang CF, Han JJ, Li YL, Ruppel A. Immunization of pigs against infection with *Schistosoma japonicum* using ultraviolet-attenuated cercariae. Parasitology 1993;106:459–62.
[20] Chen H, Nara T, Zeng X, Masao Wu SG, Fangyu WJ, Kojima YS, et al. Vaccination of domestic pig with recombinant paramyosin against *Schistosoma japonicum* in China. Vaccine 2000;20:2142–6.
[21] Pearce EJ, James SL, Hieny S, Lanar DE, Sher A. Induction of protective immunity against *Schistosoma mansoni* by vaccination with schistosome paramyosin (Sm97), a nonsurface parasite antigen. Proc Natl Acad Sci 1988;85:5678–82.
[22] Tarrab-Hazdai RF, Brenner LSV, Horowitz S, Eshhar Z, Arnon R. Protective monoclonal antibody against *Schistosoma mansoni*: antigen isolation, characterization, and suitability for active immunization. J Immunol 1985;135:2772–9.
[23] Mastin AJ, Bickle QD, Wilson RA. *Schistsoma mansoni*: migration and attrition of irradiated and challenge schistosomula in the mouse. Parasitology 1983;87:87–102.
[24] Harrop R, Wilson RA. Irradiation of *Schistsoma mansoni* cercariae impairs neuromuscular function in developing schistosomula. J Parasitol 1993;79:286–9.
[25] Jwo J, LoVerde PT. The ability of fractionated sera from animals vaccinated with irradiated cercariae of *Schistosoma mansoni* to transfer immunity to mice. J Parasitol 1989;75:252–60.
[26] Coulson PS, Wilson RA. Recruitment of lymphocytes to the lung through vaccination enhances the immunity of mice exposed to irradiated schistosomes. Infect Immun 1997;65:42–8.
[27] Hewitson JP, Hamblin PA, Mountford AP. Immunity induced by the radiation-attenuated schistosome vaccine. Parasite Immunol 2005;27:271–80.
[28] Moloney NA, Webbe G. Antibody is responsible for the passive transfer of immunity to mice from rabbits, rats or mice vaccinated with attenuated *Schistsoma japonicum* cercariae. Parasitology 1990;100:235–9.
[29] Soisson LA, Reid GD, Farah IO, Nyindo M, Strand M. Protective immunity in baboons vaccinated with a recombinant antigen or radiation-attenuated cercariae of *Schistosoma mansoni* is antibody-dependent. J Immunol 1993;151:4782–9.
[30] Kariuki TM, Farah IO, Yole DS, Mwenda JM, Van Dam GJ, Deelder AM, et al. Parameters of the attenuated schistosome vaccine evaluated in the olive baboon. Infect Immun 2004;72:5526–9.
[31] Von Lichtenberg F, Sadun EH, Cheever AW, Erickson DG, Johnson AJ, Boyce HW. Experimental infection with *Schistosoma japonicum* in chimpanzees. Am J Trop Med Hyg 1971;206:850–93.
[32] Moloney NA, Hinchcliffe P, Webbe G. Cross protection between a laboratory passaged Chinese strain of *Schistosoma japonicum* and field isolates of *S. japonicum* from China. Trans R Soc Trop Med Hyg 1989;83:83–5.
[33] Hope M, Duke M, McManus DP. A biological and immunological comparison of Chinese and Philippine *Schistosoma japonicum*. Int J Parasitol 1996;26:325–32.
[34] Hsu SYL, Hsu HF, Osborne JW. Immunization of rhesus monkeys against schistosome infection by cercariae exposed to high doses of X-radiation. Proc Soc Exp Biol Med 1969;131:1146–9.
[35] Li Hsü SY, Hsü HF, Shou Tai Xu, Hui Shi Fu, Yi Xun He, Clarke WR, et al. Vaccination against bovine schistosomiasis japonica with highly X-irradiated schistosomula. Am J Trop Med Hyg 1983;32:367–70.

[36] Hsu SYL, Xu ST, He YX, Shi FH, Shen W, Hsü HF, et al. Vaccination of bovines against schistosomiasis japonica with highly irradiated schistosomula in China. Am J Trop Med Hyg 1984;33:891–8.
[37] Watanabe K, Kikuchi M, Ohno A, Mohamed RT, Nara T, Ubaleeb R, et al. The miniature pig: a unique experimental model for *Schistosoma japonicum* infection. Parasitol Int 2004;53:293–9.
[38] Lim KC, Sun E, Bahgat M, Bucks D, Guy R, Hinz RS, et al. Blockage of skin invasion by schistosome cercariae by serine protease inhibitors. Am J Trop Med Hyg 1999;60:487–92.
[39] Basch PF. Cultivation of *Schistosoma mansoni* in vitro. I. Establishment of cultures from cercariae and development until pairing. J Parasitol 1981;67:179–85.
[40] Osada Y, Janecharut T, Hata H, Mahakunkij-Charoen Y, Chen XW, Nara T, et al. Protective immunity to *Schistosoma japonicum* infection depends on the balance of T helper cytokine responses in mice vaccinated with γ-irradiated cercariae. Parasite Immunol 2001;23:251–8.
[41] Boros DL, Warren KS. Delayed hypersensitivity-type granuloma formation and dermal reaction induced and elicited by a soluble factor isolated from *Schistosoma mansoni* eggs. J Exp Med 1970;32:488–507.
[42] Laemmli UK. Cleavage of structural proteins during the assembly of the head of bacteriophage T4. Nature 1970;227:680–5.
[43] Linke T, Ross AC, Harrison EH. Proteomic analysis of rat plasma by two-dimensional liquid chromatography and matrix-assisted laser desorption ionization time-of-flight mass spectrometry. J Chromatogr A 2006;1123:160–9.
[44] Delgado V, McLaren DJ. Evidence for enhancement of IgGI subclass expression in mice polyvaccinated with radiation-attenuated cercariae of *Schistosoma mansoni* and the role of this isotype in serum-transferred immunity. Parasite Immunol 1990;12:15–32.
[45] Simpson AJG, James TSL, Sher A. Identification of surface antigens of Schistosomula of *Schistosoma mansoni* recognized by antibodies from mice immunized by chronic infection and by exposure to highly irradiated cercariae. Infect Immun 1983;41:591–7.
[46] Dalton JP, Strand M, Mangold BL, Dean DA. Identification of *Schistsoma mansoni* glycoprotein recognized by protective antibodies from mice immunized with irradiated cercariae. J Immunol 1986;136:4689–94.
[47] Cummings RD, Nyame AK. Glycobiology of schistosomiasis. FASEB J 1996;10:838–48.
[48] Cheng GF, Lin JJ, Feng XG, Fu ZQ, Jin YM, Yuan CX, et al. Proteomic analysis of differentially expressed proteins between the male and female worm of *Schistosoma japonicum* after pairing. Proteomics 2005;5:511–21.
[49] Simpson AJ, Sher A, McCutchan TF. The genome of *Schistosoma mansoni*: isolation of DNA, its size, bases and repetitive sequences. Mol Biochem Parasitol 1982;6:125–37.
[50] McManus DP, Hu W, Brindley PJ, Feng Z, Han Z-G. Schistosome transcriptone analysis at the cutting edge. Trends Parasitol 2004;20:301–4.
[51] Ashton PD, Curwen RS, Wilson RA. Linking proteome and genome: how to identify parasite proteins. Trends Parasitol 2001;17:198–202.
[52] Fernanda JC, Olavo SP, Camila SS, Renata G-Sá, Vanderlei R. *Schistosoma mansoni* encodes SMT3B and SMT3C molecules responsible for post-translational modification of cellular proteins. Parasitol Int 2008;57:72–178.
[53] Lee H-J, Lee E-Y, Kwon M-S, Paik Y-K. Biomarker discovery from the plasma proteome using multidimensional fractionation proteomics. Curr Opin Chem Biol 2006;10:42–9.

RESEARCH LETTER

Identification of new inhibitors for alternative NADH dehydrogenase (NDH-II)

Tatsushi Mogi[1], Kazunobu Matsushita[2], Yoshiro Murase[3], Kenji Kawahara[1], Hideto Miyoshi[4], Hideaki Ui[5], Kazuro Shiomi[5], Satoshi Ōmura[5] & Kiyoshi Kita[1]

[1]Department of Biomedical Chemistry, Graduate School of Medicine, The University of Tokyo, Tokyo, Japan; [2]Department of Biological Chemistry, Faculty of Agriculture, Yamaguchi University, Yamaguchi, Japan; [3]Mycobacterium Reference Center, The Research Institute of Tuberculosis, Antituberculosis Association, Tokyo, Japan; [4]Division of Applied Life Sciences, Graduate School of Agriculture, Kyoto University, Kyoto, Japan; and [5]Kitasato Institute for Life Sciences and Graduate School of Infection Control Sciences, Kitasato University, Tokyo, Japan

Correspondence: Tatsushi Mogi, Department of Biomedical Chemistry, Graduate School of Medicine, The University of Tokyo, Bunkyo-ku, Tokyo 113-0033, Japan. Tel.: +81 3 5841 8202; fax: +81 3 5841 3444; e-mail: tmogi@m.u-tokyo.ac.jp

Received 7 October 2008; accepted 6 November 2008.
First published online 8 December 2008.

DOI:10.1111/j.1574-6968.2008.01451.x

Editor: Atsushi Yokota

Keywords
acetic acid bacteria; respiratory chain; NADH dehydrogenase; inhibitor; antibiotics.

Abstract

In bacterial membranes and plant, fungus and protist mitochondria, NADH dehydrogenase (NDH-II) serves as an alternative NADH : quinone reductase, a non-proton-pumping single-subunit enzyme bound to the membrane surface. Because NDH-II is absent in mammalian mitochondria, it is a promising target for new antibiotics. However, inhibitors for NDH-II are rare and unspecific. Taking advantage of the simple organization of the respiratory chain in *Gluconobacter oxydans*, we carried out screening of natural compounds and identified scopafungin and gramicidin S as inhibitors for *G. oxydans* NDH-II. Further, we examined their effects on *Mycobacterium smegmatis* and *Plasmodium yoelii* NDH-II as model pathogen enzymes.

Introduction

Obligate aerobe *Gluconobacter* is a genus of acetic acid bacteria that can oxidize a broad range of sugars, sugar alcohols and sugar acids. Low biomass yield and the rapid and incomplete oxidation of carbon sources (oxidative fermentation), which take place in the periplasm and is accompanied by the accumulation of products into the culture medium, make them suitable for industrial applications for bioconversion to obtain a variety of valuable products (Deppenmeier *et al.*, 2002; Adachi *et al.*, 2007). Key oxidation processes are catalyzed by dehydrogenases bound to the outer surface of the cytoplasmic membrane, and linked to the generation of proton-motive force (Matsushita *et al.*, 1994).

The recently released complete genome of *Gluconobacter oxydans* American Type Culture Collection 621H indicates that the respiratory chain lacks Complex I (NADH : quinone reductase, NDH-I), Complex II (succinate : quinone reductase) and Complex IV (cytochrome *c* oxidase) (Prust *et al.*, 2005). Genes encoding putative Complex III (quinol : cytochrome *c* reductase) and cytochrome *c* have been identified, but their functions are unclear because of the absence of cytochrome *c* oxidase. NADH produced in the cytoplasm is reoxidized by a single-subunit NADH dehydrogenase (NDH-II), a key enzyme for the regeneration of an oxidized form of NAD. NDH-II is bound peripherally to the inner surface of the cytoplasmic membrane and does not pump proton. Quinols generated by membrane-bound dehydrogenases are directly oxidized by cytochrome bo_3 oxidase (Matsushita *et al.*, 1987) and/or cyanide-insensitive oxidase (Ameyama *et al.*, 1987).

Taking advantage of the simple organization of the *Gluconobacter* respiratory chain (Matsushita *et al.*, 1994), here, we identified new inhibitors for NDH-II, which has been shown to be crucial for the adaptation of *Mycobacterium tuberculosis* (Shi *et al.*, 2005) and malaria parasite *Plasmodium* spp. (Fisher *et al.*, 2007) to host environments. From the screening of natural antibiotics in the Kitasato Institute for Life Sciences Chemical Library (Ui *et al.*, 2007),

we found the inhibitory activity of 36-membered ring macrolide scopafungin (Johnson & Dietz, 1971) and cyclic decapeptide gramicidin S (GS) (Izumiya *et al.*, 1979) (Fig. 1) for the *G. oxydans* NDH-II, and we examined their inhibitory mechanism and effects on *Mycobacterium smegmatis* and *Plasmodium yoelii* NDH-II.

Materials and methods

Preparation of bacterial membrane vesicles

Gluconobacter oxydans NBRC3172 (formerly *G. suboxydans* IFO12528) was grown aerobically in complex media containing 20 g of sodium D-gluconate, 5 g of D-glucose, 3 g of glycerol, 3 g of yeast extract and 2 g of polypepton (Nihon Pharmaceutical Co.) per 1 L using a 50-L jar fermentor at 30 °C. Cells were harvested at the late-log phase, suspended in 10 mM potassium phosphate (pH 6.0) and disrupted with a Rannie high-pressure laboratory homogenizer (model Mini-Lab, type 8.30H, Wilimington, MA). After centrifugation, to remove intact cells, the supernatant was centrifuged at 86 000 *g* for 60 min and precipitated membranes were suspended in 50 mM Tris-HCl (pH 7.4) containing 10% sucrose and 3 mM EDTA. *Mycobacterium smegmatis* mc^2155 was grown aerobically at 37 °C, and membrane vesicles were prepared from the stationary-phase cells (Kana *et al.*, 2001).

Preparation of malaria parasite mitochondria

Rodent malaria *P. yoelii* strain 17XL was injected intraperitoneally into 8-week-old female BALB/c mice, and parasite mitochondria were prepared as in Takashima *et al.* (2001). Rat liver mitochondria were prepared as in Johnson & Lardy (1967).

Enzyme assay

NADH : ubiquinone-1 (Q_1) reductase (NQR) activity of the membranes was measured at 25 °C in 100 mM Tris-HCl (pH 7.4) containing 10% sucrose, 0.02% Tween 20 (Calbiochem), 10 mM KCN and 100 μM Q_1 with a V-660 double monochromatic spectrophotometer (JASCO, Tokyo, Japan) (Mogi *et al.*, 2008), and reactions were initiated by addition of NADH ($\varepsilon_{340} = 6.3\ mM^{-1}\ cm^{-1}$, Roche) at a final concentration of 200 μM. Mitochondrial NQR and succinate : Q_1 reductase activities were determined in 50 mM potassium phosphate (pH 7.4) containing 1 mM $MgCl_2$, 0.02% Tween 20, 2 mM KCN and 100 μM Q_1 ($\varepsilon_{275} = 12.3\ mM^{-1}\ cm^{-1}$), and reactions were initiated by 200 μM NADH or 10 mM potassium succinate, respectively. NADH oxidase activity was measured in the absence of Q_1. Data analysis was carried out as in Mogi *et al.* (2008).

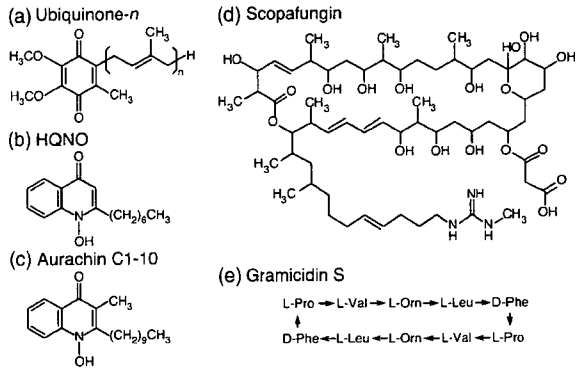

Fig. 1. Structures of ubiquinone, HQNO, aurachin C1–10, scopafungin and GS.

Materials

Synthesis of aurachin C 1-10 (Miyoshi *et al.*, 1999) was carried out as described previously. 2-Heptyl-4-hydroxyquinoline-*N*-oxide (HQNO) was obtained from Sigma.

Results and discussion

Screening of Kitasato Institute for Life Sciences Chemical Library

From the screening of a total of 304 microbial compounds (Ui *et al.*, 2007) at final concentrations of 5 $\mu g\ mL^{-1}$ with *G. oxydans* membranes, we revealed the inhibitory activities of scopafungin (niphimycin; residual activity, 33%), GS (31%), polymixin B (51%), aculeacin A (63%), funiculosin (68%) and staurosporine (70%) on 0.2 mM NADH–0.1 mM Q_1 reductase activity of NDH-II.

Inhibitors for NDH-II are rare and mostly unspecific (Kerscher, 2000). Recently, quinolone derivatives [1-hydroxy-2-dodecyl-4(1*H*)quinolone, HQNO and aurachin C] were identified as potent inhibitors for the quinone reduction site of yeast NDH-II (Eschemann *et al.*, 2005; Yamashita *et al.*, 2007). We examined the effects of quinolone inhibitors on the *G. oxydans* NDH-II and found that HQNO and aurachin C 1-10 at 10 μM reduced the NQR activity of the *G. oxydans* membranes to 28% and 12%, respectively, of the control level. Because of the limitation in the availability of isolated natural compounds, we examined further effects of scopafungin and GS (Fig. 1), which are not structurally related to ubiquinone, but showed potent inhibitory activities on the *G. oxydans* NDH-II.

Determination of 50% inhibitory concentration (IC_{50}) values for NDH-II inhibitors

We examined the dependence of the NQR activity on the concentration of GS, scopafungin, HQNO and aurachin C 1-10 and determined their IC_{50} to be 1.2 ± 0.2, 6.2 ± 0.5,

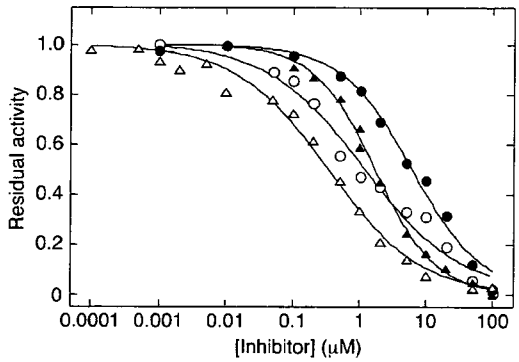

Fig. 2. Inhibition of *Gluconobacter oxydans* NDH-II by scopafungin, GS, HQNO and aurachin C 1-10. NQR activity of *G. oxydans* membranes (10 μg protein mL^{-1}) was determined in the presence of scopafungin (●), GS (○), HQNO (▲) or aurachin C1–10 (△). Data points were average values from duplicate assay. Control activity was 10.2 U mg^{-1} protein. IC_{50} values for GS, scopafungin, HQNO and aurachin C1–10 were estimated to be 1.2, 6.2, 1.7 and 0.34 μM, respectively.

1.7 ± 0.1 and 0.34 ± 0.04 μM, respectively (Fig. 2). The IC_{50} value for GS was < 3.5 μM for the *Escherichia coli bd*-type quinol oxidase (Mogi *et al.*, 2008), and the values for HQNO and aurachin C are comparable to 8 and 0.2 μM, respectively, of yeast *Saccharomyces cerevisiae* NDI1 (Yamashita *et al.*, 2007).

Kinetic analysis of inhibition of NADH-Q_1 reductase activity of NDH-II by scopafungin and GS

NADH-dependent NQR activity showed simple Michaelis–Menten kinetics with an apparent K_m value of 157 μM for NADH (at 0.2 mM Q_1) (Fig. 3). The K_m value for NADH was higher than those reported for yeast *Yarrowia lipolytica* NDE (15 μM) (Kerscher *et al.*, 1999), yeast *S. cerevisiae* NDI1 (31 μM) (de Vries & Grivell, 1988), human malaria *Plasmodium falciparum* NDH-II (17 μM) (Biagini *et al.*, 2006) and *E. coli* Ndh (34 μM) (Björklöf *et al.*, 2000). Q_1-dependent NQR activity followed Michaelis–Menten kinetics with an apparent K_m value of 16.2 ± 0.7 μM (Q_1) (Fig. 4), which is similar to 16 μM (Q_1) in *P. falciparum* (Biagini *et al.*, 2006), 5.9 μM (Q_1) in *E. coli* (Björklöf *et al.*, 2000), 6.4 μM (Q_2) in *M. tuberculosis* (Kana *et al.*, 2001) and 7 μM (decyl benzoquinone) in *Y. lipolytica* (Eschemann *et al.*, 2005).

Macrolide scopafungin and cyclic decapeptide GS (Fig. 1) are structurally unrelated to both NADH and ubiquinone, and serve as noncompetitive inhibitors ($K_i = 5.5$ and 1.4 μM, respectively) for the NADH-binding site of NDH-II (Fig. 3). Unexpectedly, scopafungin and GS were found to be a mixed-type inhibitor and a competitive inhibitor for the quinone-binding site, respectively (Fig. 4). These results

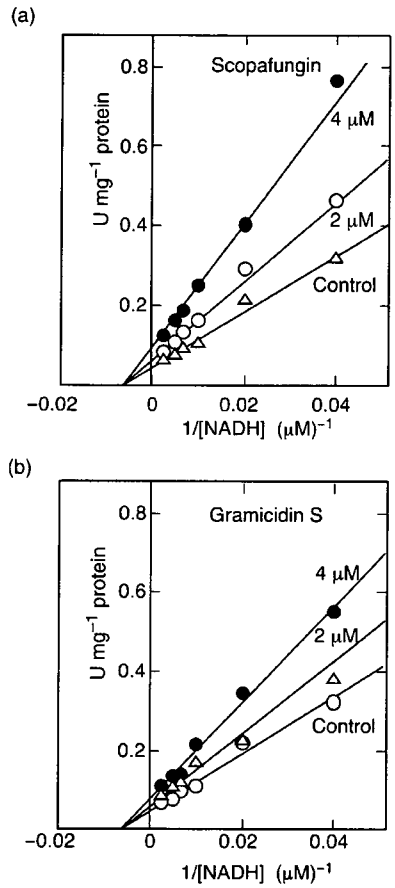

Fig. 3. Kinetic analysis of effects of scopafungin and GS on the NADH-dependent NQR activity of *Gluconobacter oxydans* NDH-II. (a) Noncompetitive inhibition by scopafungin. Apparent V_{max} values were estimated to be 19.3 (control), 17.2 (2 μM scopafungin) and 11.9 (4 μM scopafungin) U mg^{-1} protein at $K_m = 157$ μM. (b) Noncompetitive inhibition by GS. Apparent V_{max} values were determined to be 21.9 (control), 16.5 (2 μM GS) and 13.2 (4 μM GS) U mg^{-1} protein at $K_m = 157$ μM.

indicate that both compounds bind to a hydrophobic binding pocket on NDH-II molecule, which is closer to the quinone reduction site.

Effects of scopafungin and GS on *M. smegmatis* and *P. yoelii* NDH-II

Macrolide antibiotics are known to be more active against Gram-positive bacteria and fungi (Izumiya *et al.*, 1979), but targets remain to be determined while GS is active against Gram-positive and Gram-negative bacteria and several pathogenic fungi (Kondejewski *et al.*, 1996). The primary mode of the action of GS is generally assumed to perturb lipid packing, resulting in the destruction of the membrane integrity and enhancement of the permeability of the lipid bilayer (Prenner *et al.*, 1997). Very recently, we found that

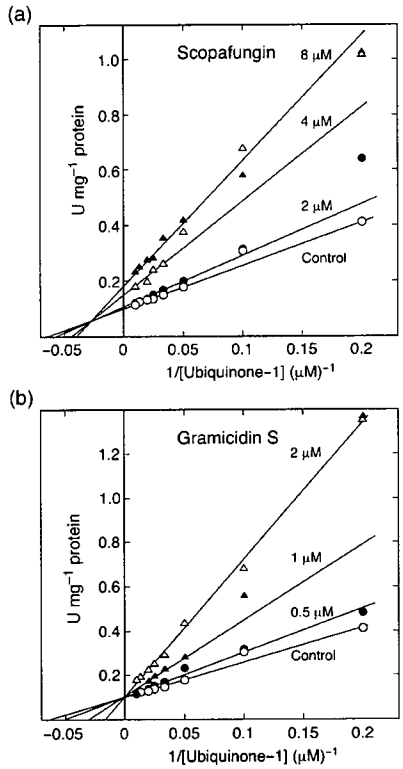

Fig. 4. Kinetic analysis of effects of scopafungin and GS on the Q_1-dependent NQR activity of *Gluconobacter oxydans* NDH-II. (a) Mixed-type inhibition by scopafungin. Apparent K_m (μM) and V_{max} (U mg^{-1} protein) values were estimated to be 15.5 and 9.6 (control), 17.4 and 9.0 (2 μM scopafungin), 22.4 and 6.5 (4 μM scopafungin) and 24.9 and 5.3 (8 μM scopafungin). (b) Competitive inhibition by GS. The apparent K_m values were determined to be 16.9 (control), 21.7 (0.5 μM GS), 37.5 (1 μM GS) and 68.3 (2 μM GS) μM at $V_{max} = 10.1$ U mg^{-1} protein.

GS can directly inhibit the *E. coli bd*-type quinol oxidase in a mixed-type manner (Mogi *et al.*, 2008). From the screening of the Kitasato Institute for Life Sciences Chemical Library with *G. oxydans* membranes, here, we identified scopafungin and GS as new inhibitors for NDH-II.

NDH-II is a promising target of new antibiotics because of the absence of NDH-II in mammalian mitochondria. The antiplasmodial activities of NDH-II inhibitors, HQNO ($IC_{50} = 3.5$ μM) (Fry *et al.*, 1990) and 1-hydroxy-2-dodecyl-4(1H) quinolone ($IC_{50} = 14$ nM) (Saleh *et al.*, 2007), have been reported previously. Thus, we examined the effects of scopafungin and GS on the NQR activity of *M. smegmatis* and rodent malaria *P. yoelii* NDH-II. At 10 μM, scopafungin showed minor effects on rat liver mitochondrial Complex I, Complex II and Complex III *plus* IV, while GS reduced NADH oxidase activity to 35% of the control by inhibiting the Complex III *plus* IV activity (Table 1). Although the IC_{50} values of scopafungin and GS for rodent malaria NDH-II were rather high (16.1 ± 3.0 and 23.0 ± 7.1 μM, respectively), both scopafungin and GS inhibited *M. smegmatis* NDH-II with IC_{50} values of 9.8 ± 0.7 and 2.0 ± 0.1 μM, respectively (Fig. 5), which are better than 12 μM of trifluoperazine for *M. tuberculosis* NDH-II (Yano *et al.*, 2006). Because scopafungin did not show severe effects on mammalian respiratory enzymes, it is a candidate for antimycobacterial agents. Here, we showed that the Kitasato Institute for Life Sciences Chemical Library (Ui *et al.*, 2007) was a powerful source for new potent antibiotics targeting to respiratory enzymes. For the identification of potential candidates, screening with recombinant NDH-IIs is currently underway in our laboratory.

Table 1. Effects of GS and scopafungin on the rat liver mitochondrial respiratory enzymes

	Relative residual activity (%)	
Enzyme activity	10 μM GS	10 μM scopafungin
NADH : Q_1 reductase (Complex I)	107	89
Succinate : Q_1 reductase (Complex II)	90	82
NADH oxidase (Complexes I+III+IV)	35	84

Control activities were 154 (NADH : Q_1 reductase), 247 (succinate : Q_1 reductase) and 102 (NADH oxidase) mU mg^{-1} protein.

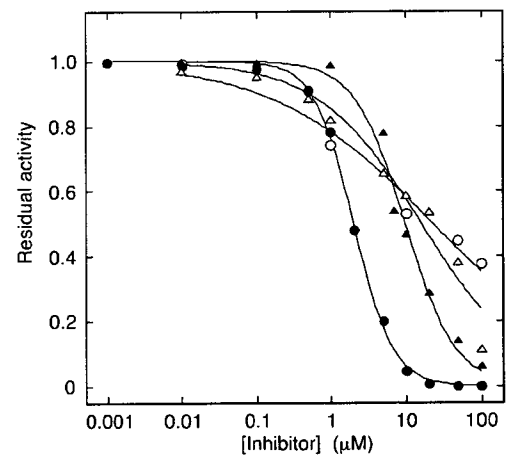

Fig. 5. Inhibition of *Mycobacterium smegmatis* and *Plasmodium yoelii* NDH-II by GS and scopafungin. Control activities of *M. smegmatis* membranes and *P. yoelii* mitochondria were 1.1 and 0.071 U mg^{-1} protein, respectively. The IC_{50} values for GS were estimated to be 2.0 (*M. smegmatis*, ●) and 23 (*P. yoelii*, ○) μM and those for scopafungin were 9.8 (*M. smegmatis*, ▲) and 16 (*P. yoelii*, △) μM.

Acknowledgements

This study was supported by a grant-in-aid for scientific research (20570124 to T.M.), scientific research on Priority Areas (18073004 to K.K.) and Creative Scientific Research (18GS0314 to K.K.) from the Japanese Ministry of Education, Science, Culture, Sports, and Technology.

References

Adachi O, Ano Y, Toyama H & Matsushita K (2007) Biooxidation with PQQ- and FAD-dependent dehydrogenases. *Modern Biooxidation, Enzymes, Reactions and Applications* (Schmid RD & Urlacher VB, eds), pp. 1–41. Wiley-VCH, Weinheim.

Ameyama M, Matsushita K, Shinagawa E & Adachi O (1987) Sugar-oxidizing respiratory chain of *Gluconobacter suboxydans*. Evidence for a branched respiratory chain and characterization of respiratory chain-linked cytochromes. *Agr Biol Chem* **51**: 2943–2950.

Biagini GA, Viriyavejakul P, O'Neill PM, Bray PG & Ward SA (2006) Functional characterization and target validation of alternative Complex I of *Plasmodium falciparum* mitochondria. *Antimicrob Agents Ch* **50**: 1841–1851.

Björklöf K, Zickermann V & Finel M (2000) Purifiction of the 45 kDa, membrane bound NADH dehydrogenase of *Escherichia coli* (NDH-2) and analysis of its interaction with ubiquinone analogs. *FEBS Lett* **467**: 105–110.

Deppenmeier U, Hoffmeister M & Prust C (2002) Biochemistry and biotechnological applications of *Gluconobacter* strains. *Appl Microbiol Biot* **60**: 233–242.

De Vries S & Grivell LA (1988) Purification and characterization of a rotenone-insensitive NADH : Q_6 oxidoreductase from mitochondria of *Saccharomyces cerevisiae*. *Eur J Biochem* **176**: 377–341.

Eschemann A, Galkin A, Oettmeier W, Brandt U & Kerscher S (2005) HDQ (1-hydroxy-2-dodecyl-4(1*H*)quinolone), a high affinity inhibitor for mitochondrial alternative NADH dehydrogenase: evidence for a ping-pong mechanism. *J Biol Chem* **280**: 3138–3142.

Fisher N, Bray PG, Ward SA & Biagini GA (2007) The malaria parasite type II NADH : quinone oxidoreductase: an alternative enzyme for an alternative lifestyle. *Trends Parasitol* **23**: 305–310.

Fry M, Webb E & Pudney M (1990) Effect of mitochondrial inhibitors on adenosine triphosphate levels in *Plasmodium falciparum*. *Comp Biochem Physiol* **B96**: 775–782.

Izumiya N, Kato T, Aoyaga H, Waki M & Kondo M (1979) *Synthetic Aspects of Biologically Active Cyclic Peptides: Gramicidin S and Tyrocidines*. Halsted Press, New York.

Johnson D & Lardy H (1967) Isolation of liver or kidney mitochondria. *Methods in Enzymology, Vol. 10* (Estabrook RW & Pullman ME, eds), pp. 94–96. Academic Press, New York.

Johnson LE & Dietz A (1971) Scopafungin, a crystalline antibiotic produced by *Streptomyces hygroscopicus* var. *enhygrus* var. *nova*. *Appl Microbiol* **22**: 303–308.

Kana BD, Weinstein EA, Avarbock D, Dawes SS, Rubin H & Mizrahi V (2001) Characterization of the *cydAB*-encoded cytochrome *bd* oxidase from *Mycobacterium smegmatis*. *J Bacteriol* **183**: 7076–7086.

Kerscher SJ (2000) Diversity and origin of alternative NADH : ubiquinone oxidoreductase. *Biochim Biophys Acta* **1459**: 274–283.

Kerscher SJ, Okun JG & Brandt U (1999) A single external enzyme confers alternative NADH : ubiquinone oxidoreductase activity in *Yarrowia lipolytica*. *J Cell Sci* **112**: 2347–2354.

Kondejewski LH, Farmer SW, Wishart D, Kay CM, Hancock REW & Hodges RS (1996) Modulation of structure and antibacterial and hemolytic activity by ring size in cyclic gramicidin S analogs. *J Biol Chem* **271**: 25261–25268.

Matsushita K, Shinagawa E, Adachi O & Ameyama M (1987) Purification and characterization of cytochrome *o*-type oxidase from *Gluconobacter suboxydans*. *Biochim Biophys Acta* **894**: 304–312.

Matsushita K, Toyama H & Adachi O (1994) Respiratory chains and bioenergetics of acetic acid bacteria. *Advances in Microbial Physiology, Vol. 36* (Rose AH & Tempest DW, eds), pp. 247–301. Academic Press Ltd, London.

Miyoshi H, Takegami K, Sakamoto K, Mogi T & Iwamura H (1999) Characterization of the ubiquinol oxidation sites in cytochromes *bo* and *bd* from *Escherichia coli* using aurachin C analogues. *J Biochem* **125**: 138–142.

Mogi T, Ui H, Shiomi K, Ômura S & Kit K (2008) Gramicidin S identified as a potent inhibitor for cytochrome *bd*-type quinol oxidase. *FEBS Lett* **582**: 2299–2302.

Prenner EJ, Lewis RNAH, Newman KC, Gruner SM, Kondejewski LH, Hodges RS & McElhaney RN (1997) Nonlamellar phases induced by the interaction of gramicidin S with lipid bilayers. A possible relationship to membrane disrupting activity. *Biochemistry* **36**: 7906–7916.

Prust C, Hoffmeister M, Liesegang H, Wiezer A, Fricke WF, Ehrenreich A, Gottschalk G & Deppenmeier U (2005) Complete genome sequence of the acetic acid bacterium *Gluconobacter oxydans*. *Nat Biotechnol* **23**: 195–200.

Saleh A, Friesen J, Baumeister S, Gross G & Bohne W (2007) Growth inhibition of *Toxoplasma gondii* and *Plasmodium falciparum* by nanomolar concentrations of 1-hydroxy-2-dodecyl-4(1*H*)quinolone, a high-affinity inhibitor of alternative (type II) NADH dehydrogenases. *Antimicrob Agents Ch* **51**: 1217–1222.

Shi L, Sohaskey CD, Kana BD, Dawes S, North RJ, Mizrahi V & Gennaro ML (2005) Changes in energy metabolism of *Mycobacterium tuberculosis* in mouse lung and under *in vitro* conditions affecting aerobic respiration. *P Natl Acad Sci USA* **102**: 15629–15634.

Takashima E, Takamiya S, Takeo S, Mi-ichia F, Amino H & Kita K (2001) Isolation of mitochondria from *Plasmodium falciparum* showing dihydroorotate dependent respiration. *Parasitol Int* **50**: 273–278.

Ui H, Ishiyama A, Sekiguchi H, Namatame M, Nishihara A, Takahashi A, Shiomi K, Otoguro K & Ômura S (2007) Selective and potent *in vitro* antimalarial activities found in four microbial metabolites. *J Antibiot* **60**: 220–222.

Yamashita T, Nakamaru-Ogiso E, Miyoshi H, Matsuo-Yagi A & Yagi T (2007) Roles of bound quinone in the single subunit NADH–quinone oxidoreductase (Ndi1) from *Saccharomyces cerevisiae*. *J Biol Chem* **282**: 6012–6020.

Yano T, Li L-S, Weinstein E, The J-S & Rubin H (2006) Steady-state kinetics and inhibitory action of antitubercular phenothiazines on *Mycobacterium tuberculosis* type-II NADH-menaquinone oxidoreductase (NDH-2). *J Biol Chem* **281**: 11456–11463.

J. Biochem. 2009;145(2)229–237
doi:10.1093/jb/mvn161

Mitochondrial Dehydrogenases in the Aerobic Respiratory Chain of the Rodent Malaria Parasite *Plasmodium yoelii yoelii*

Kenji Kawahara[1], Tatsushi Mogi[1,*], Takeshi Q Tanaka[1], Masayuki Hata[1], Hideto Miyoshi[2] and Kiyoshi Kita[1,†]

[1]Department of Biomedical Chemistry, Graduate School of Medicine, the University of Tokyo, Hongo, Bunkyo-ku, Tokyo 113-0033; and [2]Division of Applied Life Sciences, Graduate School of Agriculture, Kyoto University, Sakyo-ku, Kyoto 606-8502, Japan

Received October 7, 2008; accepted November 19, 2008; published online December 6, 2008

In the intraerythrocytic stages of malaria parasites, mitochondria lack obvious cristae and are assumed to derive energy through glycolysis. For understanding of parasite energy metabolism in mammalian hosts, we isolated rodent malaria mitochondria from *Plasmodium yoelii yoelii* grown in mice. As potential targets for antiplasmodial agents, we characterized two respiratory dehydrogenases, succinate:ubiquinone reductase (complex II) and alternative NADH dehydrogenase (NDH-II), which is absent in mammalian mitochondria. We found that *P. y. yoelii* complex II was a four-subunit enzyme and that kinetic properties were similar to those of mammalian enzymes, indicating that the *Plasmodium* complex II is favourable in catalysing the forward reaction of tricarboxylic acid cycle. Notably, *Plasmodium* complex II showed IC_{50} value for atpenin A5 three-order of magnitudes higher than those of mammalian enzymes. Divergence of protist membrane anchor subunits from eukaryotic orthologs likely affects the inhibitor resistance. Kinetic properties and sensitivity to 2-heptyl-4-hydroxyquinoline-*N*-oxide and aurachin C of NADH: ubiquinone reductase activity of *Plasmodium* NDH-II were similar to those of plant and fungus enzymes but it can oxidize NADPH and deamino-NADH. Our findings are consistent with the notion that rodent malaria mitochondria are fully capable of oxidative phosphorylation and that these mitochondrial enzymes are potential targets for new antiplasmodials.

Key words: complex II, inhibitor, mitochondria, NDH-II, rodent malaria.

Abbreviations: AC, aurachin C; DCIP, 2,4-dichlorophenolindophenol; DHO, dihydroorotate; DHOD, DHO dehydrogenase; HQNO, 2-heptyl-4-hydroxyquinoline-*N*-oxide; hrCNE, high-resolution clear-native electrophoresis; IC_{50}, the 50% inhibitory concentration; NBT, nitro blue tetrazolium chloride; NDE, NDH-II bound to the outer surface of the mitochondrial inner membrane; NDI, NDH-II bound to the matrix side of the mitochondrial inner membrane; NQR, NADH:quinone reductase; Q_n, ubiquinone-n; SDH, succinate dehydrogenase; SQR, succinate:quinone reductase; TCA, tricarboxylic acid.

INTRODUCTION

Malaria remains one of the main global health problems, causing more than 1 million deaths per year, with about 90% of deaths and 60% of cases occurring in Africa, south of the Sahara (*1*). Mortality associated with malaria is mainly caused by the erythrocytic stage cells of human malaria *Plasmodium falciparum*. The emerging resistance against established drugs in *Plasmodium* populations (*2*) emphasizes the urgent need for the development of new antiplasmodial drugs.

Energy metabolism of *Plasmodium* is quite different from that of mammalian hosts. Intraerythrocytic stages of parasites have been considered for a long time to rely on incomplete oxidation of glucose with secretion of end products such as lactate and pyruvate (*3*) and to possess mitochondria that lack oxidative phosphorylation and a functional tricarboxylic acid (TCA) cycle (*4*, *5*). *Plasmodium* spp. lacks genes coded for the proton-translocating NADH dehydrogenase (NDH-I, complex I) present in mammalian mitochondria (*6*, *7*) and uses a rotenone-insensitive single-subunit NADH dehydrogenase (NDH-II) (*8*), which is assumed not to oxidize deamino-NADH (*9*). Succinate:ubiquinone oxidoreductase (complex II, succinate dehydrogenase (SDH)) is a membrane-bound TCA cycle enzyme and consists of four subunits: a flavoprotein subunit (Fp, SDH1) and an iron–sulphur subunit (Ip, SDH2) form a soluble heterodimer, which binds to a membrane anchor *b*-type cytochrome [CybL (SDH3)/CybS (SDH4) heterodimer]. The *Plasmodium SDH1* and *SDH2* genes have been cloned by homology probing (*10*) while SDH3 and SDH4 appear highly divergent from orthologs and are still not annotated in the current database (*6*, *7*). Membrane bound subuniuts *a* and *b* of ATP synthase also remain unidentified (*6*, *7*), and thus complete mitochondrial ATP synthase was assumed to be absent in *Plasmodium* spp. (*4*, *5*, *11–13*). Recently, Painter *et al.* (*13*) claimed that

*To whom correspondence addressed. Tel: +81-3-5841-3526, Fax: +81-3-5841-3444, E-mail: tmogi@m.u-tokyo.ac.jp
†Correspondence may also be addressed. Tel: +81-3-5841-3526, Fax: +81-3-5841-3444, E-mail: kitak@m.u-tokyo.ac.jp

the mitochondrial respiratory chain is required only for the regeneration of an oxidized form of ubiquinone, which serves as the electron acceptor for type 2 dihydroorotate dehydrogenase (DHOD), an essential enzyme for pyrimidine biosynthesis. It is widely accepted that the majority of the parasite's ATP demand is met through glycolysis (*11*).

On the contrary, atovaquone, an inhibitor for ubiquinol:cytochrome *c* reductase (complex III) (*14*), showed the antiplasmodial activity for *P. falciparum* with the 50% inhibitory concentration (IC_{50}) of 1 nM (*15*) and collapsed the mitochondrial membrane potential in *P. yoelii yoelii* (*16*). Uyemura *et al.* (*8*, *17*) demonstrated oxidative phosphorylation and succinate respiration in trophozoites of rodent malaria parasites. These observations suggest that *Plasmodium* mitochondria possess all subunits for canonical complex II and ATP synthase and are fully capable of oxidative phosphorylation.

It was shown recently that metabolism in *P. falciparum* parasites grown in human patients is affected by varied oxygen and substrate levels and by host-parasite interactions (*18*). The authors found the induction of gene sets associated with oxidative phosphorylation including respiratory enzymes. For understanding energy metabolism in malaria parasites, the isolation of active mitochondria from parasites, which have been adapted to host environments, is essential. In this study, *P. y. yoelii* mitochondria were isolated from parasites grown in mouse erythrocytes and enzymatic properties of complex II and NDH-II were characterized. Two-dimensional PAGE analysis supports the presence of membrane anchors in *Plasmodium* complex II. These findings indicate that *Plasmodium* mitochondria are fully capable of succinate-dependent oxidative phosphorylation as suggested by previous observations (*8*, *17*). Because the difference in the inhibitor sensitivity of complex II between *Plsamodium* and mammalian enzymes and the absence of NDH-II in mammalian mitochondria, these two enzymes are promising targets for new antimaralials.

MATERIALS AND METHODS

Parasite Culture—Animal care and experimental procedures were performed according to the Guidelines for Animal Experimentation, the University of Tokyo. *P. y. yoelii* strain 17XL was a kind gift of H. Otsuki (Ehime University). This strain can rapidly propagate without cerebral malaria and does not infect reticulocytes. About 3.0×10^7 parasites were injected intraperitoneally to 8-week-old female BALB/c mice, and the developmental stage and parasitemia were monitored by examination of Giemsa-stained thin blood smears. About 7.5 ml of the blood was collected from 10 mice by cardiac puncture 130–140 h after infection. To remove leukocytes and platelets, the blood was mixed with 0.5 ml of heparine and passed over a powdered cellulose column (CF11; Whatman, Clifton; 0.5 ml/ml blood), which has been equilibrated with 20 ml of PBS (*19*). Erythrocytes were eluted with 30 ml of PBS and collected by centrifugation at 4°C at $800 \times g$ for 5 min. In control experiments with uninfected mice, microscopic observations and examination of complex II and dihydroorotate dehydrogenase (DHOD) activities excluded the possible contamination of mouse leukocytes in the eluate. Erythrocytes were washed three times with RPMI-1640 medium (Gibco) and then transferred to RPMI-1640 medium supplemented with 10% AlbuMax I (Gibco) at the hematoclit of 3%. Then erythrocytes were incubated at 37°C for 2 h under conditions of 90% N_2, 5% O_2 and 5% CO_2, and trophozoite-rich parasites were recovered by centrifugation as above.

Preparation of Mitochondria—To isolate parasites, infected erythrocytes were lysed for 10 min on ice with 0.1% (w/v) saponin and the lysate was centrifuged at 4°C at $2,380 \times g$ for 10 min to remove erythrocyte membranes. Parasites were washed twice with PBS by centrifugation at 4°C at $5,800 \times g$ for 10 min and resuspended with 10–20 ml of buffer A [225 mM mannitol, 75 mM sucrose, 5 mM $MgCl_2$, 5 mM KH_2PO_4, 5 mM HEPES, 1 mM EGTA (pH 7.4)], supplemented with 0.1% (w/v) fatty acid-free bovine serum albumin (PAA Cell Culture Co.), 1 mM phenylmethanesufonyl fluoride (Sigma) and 1 × Protease Inhibitor Cocktail for general use (Sigma). Parasites were disrupted by N_2 cavitation at 1,200 psi for 20 min with 4639 Cell Disruption Bomb (Parr, USA) (*20*). Lysate was centrifuge at 4°C at $700 \times g$ for 8 min, and the resultant precipitate containing unbroken parasites was resuspended with 10 ml of buffer A and disrupted as above. This procedure was repeated twice to improve the parasite yield. Crude mitochondria were recovered from the supernatant by centrifugation at 4°C at $10,000 \times g$ for 8 min and suspended in buffer A at ~5 mg protein/ml. Rat liver mitochondria were prepared as described by Johnson and Lardy (*21*).

Enzyme Assay—Enzyme assay was performed at 25°C with V-660 double monochromatic spectrophotometer (JASCO, Tokyo, Japan; <0.00005 Abs noise) or UV-3000 double wavelength spectrophotometer (Shimadzu Corp., Kyoto, Japan), and reactions were started by addition of substrates (electron donors). Succinate:quinone reductase (SQR) activity was determined as quinone-mediated succinate:2,4-dichlorophenolindophenol (DCIP) reductase in 50 mM potassium phosphate (pH 8.0) containing 10 mM potassium succinate, 100 μM ubiquinone-2 (Q_2) and 45 μM DCIP ($\varepsilon_{600} = 21\ mM^{-1}\ cm^{-1}$) in the presence of 2 mM KCN. NADH:ubiquinone reductase (NQR) activity was measured in 50 mM potassium phosphate (pH 8.0) containing 200 μM NADH ($\varepsilon_{340} = 6.22\ mM^{-1}\ cm^{-1}$) and 100 μM ubiquinone-1 (Q_1) in the presence of 10 μM atovaquone and 2 mM KCN (*15*). DHOD activity was measured as DHO:DCIP reductase in 30 mM Tris–HCl (pH 8.0) containing 500 μM DHO, 100 μM Q_2 and 45 μM DCIP in the presence of 2 mM KCN (*20*). DHO:cytochrome *c* reductase activity was determined with 20 μM horse cytochrome *c* ($\varepsilon_{550} = 19\ mM^{-1}\ cm^{-1}$) in place of 45 μM DCIP (*20*). For inhibition studies, the reaction mixture was preincubated for 5 min in the presence of 0.1% (w/v) sucrose monolaurate (Mitsubishi-Kagaku Foods Co., Tokyo, Japan) to disperse hydrophobic substrates and inhibitors. Kinetic analysis and the estimation of the 50% inhibitory concentration (IC_{50}) were performed as described previously (*22*).

Clear-Native Electrophoresis and Activity Staining—Mitochondria were precipitated at 4°C at 20,400 × *g* for 5 min and resuspended at 6 mg protein/ml in 10 mM Tris–HCl (pH 7.4) containing 1% sucrose monolaurate, 1 mM sodium malonate and Protease Inhibitor Cocktail by brief sonication. After 20 min incubation at 4°C with rotating, the mixture was centrifuged at 4°C at 107,000 × *g* for 30 min and supernatant was concentrated at 4°C at 4,000 × *g* with Nanosep ultrafiltration devices (MWCO 100,000, Pall Life Science). Solubilized mitochondrial proteins were subjected to high resolution clear-native electrophoresis (hrCNE) (*23*) with 3–12% Novex gels (Invitrogen) using 0.02% dodecylmaltoside and 0.05% sodium deoxycholate for the cathode buffer additives. Gels were incubated at 25°C for 10 min in 30 mM Tris–HCl (pH 7.4) containing 20 mM potassium succinate and 0.5 mM nitro blue tetrazolium chloride (NBT), and then complex II band was visualized by 1 h incubation in dark in the presence of 0.2 mg/ml phenazine methosulphate. Protein bands were stained with GelCode (Pierce).

Analysis of Membrane Anchor Subunits of Complex II—Complex II bands identified as succinate:NBT reductase in hrCNE were cut out from gels and equilibrated with an equal amount of 2× SDS–PAGE sample buffer. Gel pieces were applied to 10–20% Supersep gels (Wako Pure Chemicals, Tokyo, Japan) and SDS–PAGE analysis was carried out. Protein bands were visualized by silver staining.

Miscellaneous—Protein contents of mitochondria and solubilized membrane proteins were determined with BIO-RAD and BCA protein assay reagent (Pierce), respectively, using bovine serum albumin as standard. Western blot analysis was carried out using anti-*P. falcifaum* (Pf) Fp and anti-PfIp rabbit antiserum and cross-reacted bands were visualized by alkaline phosphatase-conjugated anti-rabbit IgG (Bio-Rad) (*24*).

RESULTS

Preparation of Plasmodium Mitochondria—After infection of mice with rodent malaria parasites, we monitored amounts of erythrocytes and parasitemia and found that the number of parasites decreased sharply 140 h after infection as the number of the erythrocyte decreased. Thus, we collected the infected blood 130 to 140 h after infection. Leukocyte-free washed erythrocytes were incubated at 37°C for 2 h in RPMI-1640 medium supplemented with 10% AlbuMax I to adjust the developmental stage to trophozoites (trophozoite : ring : schizont = 7 : 2 : 1). Then the parasites were released from infected erythrocytes with 0.1% saponin and disrupted by the N_2 cavitation method (*20*).

Yield of Plasmodium Mitochondria—SQR activity and DHOD activity of *P. y. yoelii* mitochondria were 5- and 3-fold, respectively, higher than those of the axenic cultured *P. falciparum* (*20*). Furthermore, yields of mitochondrial proteins (5.5 ± 1.3 mg protein) and total activities of complex II (56 ± 14 mU) and DHOD (132 ± 18 mU) after preparation from ten infected mice were much greater than those of *P. falciparum* mitochondria [1 mg protein, 2 mU (*25*), and 7 mU (*20*), respectively, from the 360-ml *in vitro* culture]. Thus, in terms of the yield and specific activity, *P. y. yoelii* mitochondria are suitable for biochemical studies on mitochondrial enzymes of malaria parasites.

Table 1. **Enzymatic properties of *P. y. yoelii* mitochondria.**

Enzyme	Specific activity (mU/mg protein)	
	P. y. yoelii[a]	Rat liver
Succinate:DCIP reductase (complex II)	2.66 ± 0.02	188
NADH:Q_1 reductase[b]	42.2 ± 0.3	152
NADH:Cyt *c* reductase[c]	18.6 ± 1.6	ND[d]
DHO:DCIP reductase (DHOD)	10.5 ± 1.3	2.6
Q_1H_2 oxidase (complex III + complex IV)	19.4 ± 0.2	166

[a]Values were mean ± SD. Freshly prepared *P. y. yoelii* mitochondria showed SQR, NQR and DHOD activities of 10.2 ± 0.1, 63.2 ± 10.1 and 24.1 ± 3.9 mU/mg protein (n = 6), respectively. Enzyme activities were reduced to about one half after freeze-thaw of mitochondria preparations, which have been stored at −80°C. [b]NDH-II of *P. y. yoelii* or NDH-I of rat liver mitochondria were analysed. [c](NDH-II of *P. y. yoelii* or NDH-I of rat liver mitochondria) + complex III were analysed. [d]ND, not determined.

Comparison of Mitochondrial Enzymes from P. y. yoelii and Rat Liver—When comparing with rat liver mitochondria, SQR (complex II), NQR (NDH-II) and Q_1H_2 oxidase (complex III *plus* complex IV) activity of *P. y. yoelii* mitochondria were 1.4%, 28% and 12%, respectively, of rat liver mitochondria whereas DHOD activity was 4-fold higher than that of rat liver mitochondria (Table 1). Rotenone [IC_{50} = 13 nM for bovine complex I (*26*)] inhibited rat liver mitochondria complex I 95–97% at 1 μM while the inhibition of the *P. y. yoelli* NQR activity by 10 μM rotenone was only 20%. Since NQR activity of *P. y. yoelii* mitochondria followed a simple Michaelis–Menten kinetics (see below), we concluded that the enzyme activities are not due to contaminated mouse mitochondria derived from leukocytes or platelets.

Enzymatic Properties of Plasmodium Complex II—SQR activity of *P. y. yoelii* mitochondria displayed Michaelis–Menten kinetics (Fig. 1). Apparent K_m values for succinate and Q_2 were estimated to be 49 and 0.17 μM, respectively, which are close to 20 and 0.5 μM, respectively, of bovine complex II (*27*). Apparent K_m value for Q_1 was found to be 1.6 μM. Differences in K_m value (9-fold) and V_{max}/K_m ratio (19-fold) between Q_1 and Q_2 indicate that the 6-polyprenyl tail of the ubiquinone ring contributes to the binding affinity and that Q_2 is better substrate than Q_1.

Then effects of the quinone-binding site inhibitors on the SQR activity were examined. Atpenin A5 and carboxin are known inhibitors for bovine complex II with IC_{50} values of 4 nM and 1 μM, respectively (*28*) and plumbagin (5-hydroxy-2-methyl-1,4-naphthoquinone) has been reported to inhibit *P. falciparum* complex II (IC_{50} = 5 μM) and the growth (IC_{50} = 0.27 μM) (*29*). At 100 μM Q_2, we found that IC_{50} values for atpenin A5 and carboxin were 4.6 and 3.6 μM, respectively, in *P. y. yoelii* mitochondria and 7.1 nM and 3.8 μM, respectively, in rat liver mitochondria (Fig. 2). The inhibition by plumbagin was only 50% even at 100 μM.

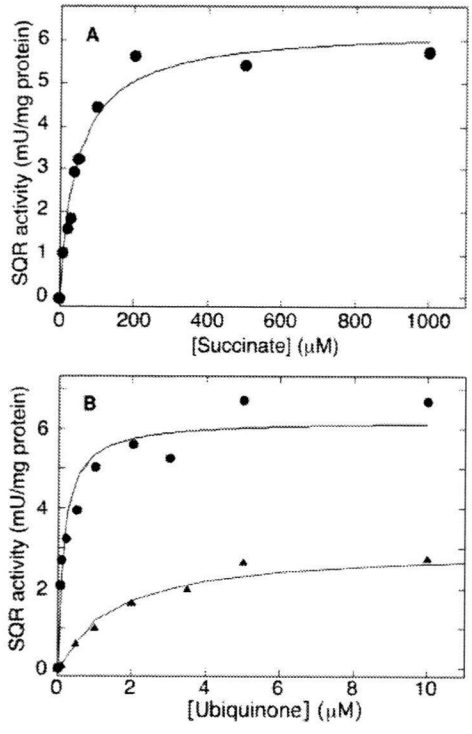

Fig. 1. **Kinetic analysis of SQR activity of *P. y. yoelii* mitochondria.** (A) As a function of the succinate concentration, SQR activity was examined at 6 μg mitochondrial protein/ml in the presence of 0.1 mM Q_2. Data points were averages from three independent preparations (6.19 ± 0.93 mU/mg protein with 1 mM succinate and 0.1 mM Q_2). Data were fitted to Michaelis–Menten kinetics with apparent K_m and V_{max} values of 49.3 ± 7.0 μM and 6.26 ± 0.27 mU/mg protein, respectively. (B) As a function of the Q_1 (circles) or Q_2 (triangles) concentration, SQR activity was examined in the presence of 10 mM succinate. Data points were averages from two independent preparations (6.25 ± 0.87 mU/mg protein with 1 mM succinate and 0.1 mM Q_2). Data were fitted to Michaelis–Menten kinetics with apparent K_m and V_{max} values of 1.61 ± 0.20 μM and 3.03 ± 0.12 mU/mg protein, respectively, for Q_1 and 0.17 ± 0.04 μM and 6.20 ± 0.30 mU/mg protein, respectively, for Q_2.

Membrane Anchor Subunits of Plasmodium Complex II—For reduction of ubiquinone, *Plasmodium* complex II should have a quinone-binding pocket provided by Ip and the CybL/CybS heterodimer (*30–32*). For the examination of subunit structure of *Plasmodium* complex II, we first determined the molecular weight of *P. y. yoelii* complex II by hrCNE, followed by in-gel activity staining as phenazine methosulphate-mediated succinate : NBT reductase. An apparent molecular weight of *P. y. yoelii* complex II was estimated to be 135 kDa (Fig. 3, lane 2), which is comparable to 130 kDa of bovine and yeast complex II (*33*). Western blot analysis identified Fp and Ip as the 70- and 35-kDa proteins, respectively (Fig. 3, lanes 3 and 4), indicating that a sum of molecular weights of membrane anchor subunits is about 30 kDa. Subsequently, the 135-kDa bands in hrCNE were excised from gels and subjected to SDS–PAGE analysis. Due to an extremely low activity of *Plasmodium* complex II (~1% of mammalian mitochondria) and the diffusion of a reduced product of NBT, it was difficult to cut out the complex II band but we were able to identify 70, 35, 16 and 14 kDa bands as putative subunits of the 135-kDa complex (Fig. 3, lane 5).

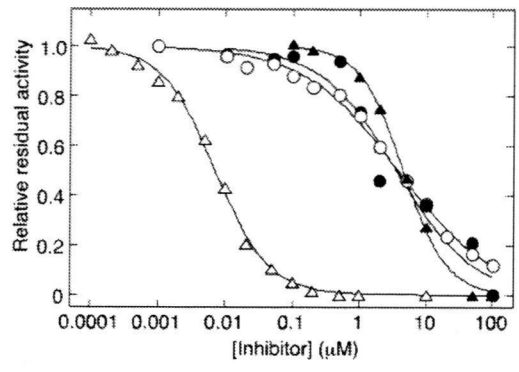

Fig. 2. **Inhibition of SQR activity of *P. y. yoelii* mitochondria by atpenin A5 and carboxin.** SQR activity of *P. y. yoelii* (closed symbols) and rat liver (open symbols) mitochondria was determined with 10 mM potassium succinate and 0.1 mM Q_2 in the presence of atpenin A5 (triangles), and carboxin (circles). Data points were average values from two independent preparations. IC_{50} values were determined to be 4.6 ± 0.2 μM for atpenin A5 and 3.6 ± 1.0 μM for carboxin in *P. y. yoelii* mitochondria and 7.1 ± 0.3 nM for atpenin A5 and 3.8 ± 0.1 μM for carboxin in rat liver mitochondria. Control activitiy of *P. y. yoelii* mitochondria was 2.68 ± 0.03 mU/mg protein.

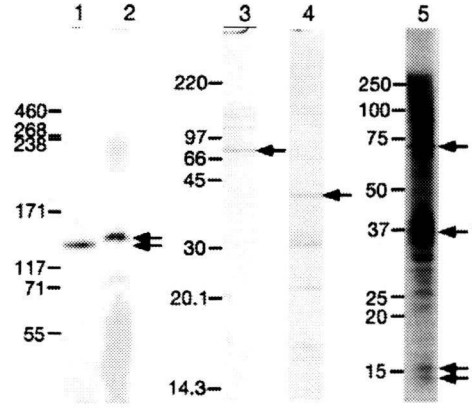

Fig. 3. **Electrophoresis analysis of complex II in *P. y. yoelii* mitochondria.** Solubilized mitochondrial proteins were subjected to hrCNE, and complex II of bovine (lane 1, 2.4 μg protein) and *P. y. yoelii* (lane 2, ~0.4 mg protein) mitochondria were visualized by SDH activity staining. Arrows indicate complex II bands. For Western blot analysis, 10 μg of mitochondrial proteins were subjected to 15% SDS–PAGE and Fp (lane 3) and Ip (lane 4), indicated by arrows, were identified by anti-PfFp and anti-PfIp rabbit antisera, respectively. For identification of *P. y. yoelii* complex II subunits, complex II bands in hrCNE were excised from gels and subjected to 10–20% SDS–PAGE, followed by silver staining (lane 5). Putative subunits of *P. y. yoelii* complex II are indicated by arrows. HiMark Prestained High Molecular Weight Protein Standard (Invitrogen), Rainbow Colored Protein Molecular Weight Marker (High molecular weight range) (Amersham Pharmacia Biotech), and Precision Plus Protein Standard (Bio-Rad) were used as molecular weight standards for lanes 1 and 2, lanes 3 and 4, and lane 5, respectively.

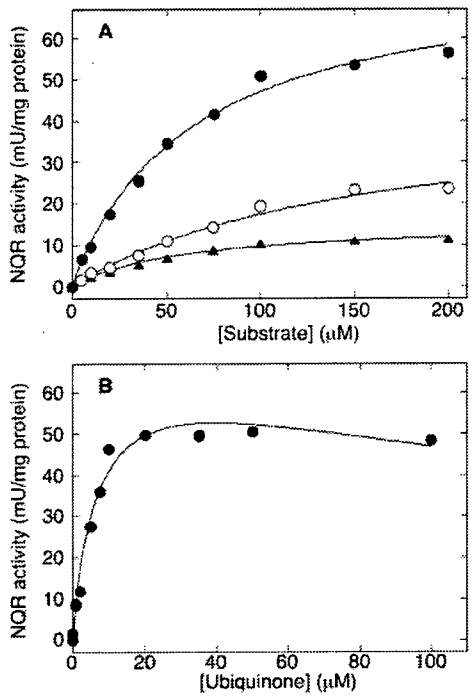

Fig. 4. **Kinetic analysis of NQR activity in *P. y. yoelii* mitochondria.** (A) As a function of the concentration of NADH (closed circle), NADPH (open circle) or deamino-NADH (closed triangle), NQR activity was examined at 6 μg protein/ml in the presence of 0.1 mM Q_1. Data points were averages from two independent preparations (44.9 ± 4.8 mU/mg protein with 0.2 mM NADH). Data were fitted to Michaelis–Menten kinetics with apparent K_m and V_{max} values of 63.2 ± 6.9 μM and 76.7 ± 3.4 mU/mg protein, respectively, for NADH, 157 ± 33 μM and 44.4 ± 5.4 mU/mg protein, respectively, for NADPH, 58.4 ± 5.7 μM and 15.1 ± 0.6 mU/mg protein, respectively, for deamino-NADH. (B) As a function of the concentration of Q_1, NQR activity was examined in the presence of 0.2 mM NADH. Data points were average values from two independent preparations [48.6 ± 7.9 mU/mg protein at 0.1 mM Q_1). Data were fitted to substrate inhibition kinetics with apparent K_m, V_{max} and K_{is} values of 7.2 ± 1.7 μM, 71.8 ± 7.6 mU/mg protein, and 218 ± 97 μM, respectively, using the equation $v = V_{max}$ $S/(K_m + S + S\ (1+S/K_{is}))$.

Enzymatic Properties of Plasmodium NDH-II—*Plasmodium* spp. lacks genes encoding complex I (*6*, *7*) and uses a single-subunit NADH dehydrogenase (NDH-II) (*8*, *15*). Upon permealization of mitochondria with 30 μg/ml alamethicin, which forms pores large enough to permit the rapid diffusion of NADH (*34*), NQR and SQR activities increased 32% and 27%, respectively, indicating that *Plasmodium* NDH-II is likely located at the matrix side of the inner membrane.

When reactions were started by addition of NADH, NQR activity showed a simple Michaelis–Menten kinetics with apparent K_m and V_{max} values of 63 μM for NADH and 77 mU/mg protein, respectively (Fig. 4A). K_m value for NADH was closer to 31 μM of *Saccharomyces cerevisiae* internal NDH-II (NDI1) (*35*) and 34 μM of *E. coli* NDH-II (*36*) than 15 μM of yeast *Yarrowia lipolytica* external NDH-II (NDE) (*37*). In contrast,

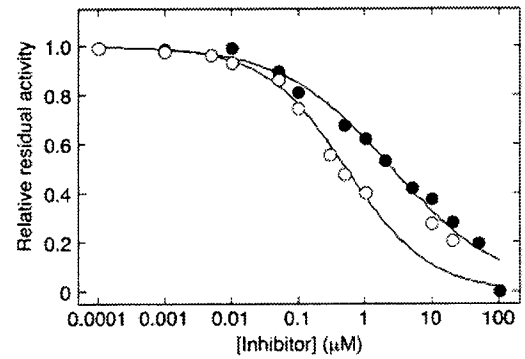

Fig. 5. **Inhibition of NQR activity of *P. y. yoelii* mitochondria by HQNO and Aurachin C1-10.** NQR activity of *P. y. yoelii* mitochondria was determined with 0.2 mM NADH and 0.1 mM Q_1 in the presence of HQNO (closed circle) or aurachin C1-10 (open circle). Data points were average values from two independent preparations. Control activity of *P. y. yoelii* mitochondria was 45.6 ± 1.3 mU/mg protein with 0.1 mM Q_1. IC_{50} values for HQNO and aurachin C1-10 were estimated to be 2.5 ± 0.4 and 0.47 ± 0.03 μM, respectively.

Q_1-started NQR activity showed substrate inhibition kinetics with K_m and K_{is} values of 7 and 218 μM, respectively, for Q_1 (Fig. 4B). Unlike *E. coli* NADH-II (*36*) and *Y. lipolytica* NDE (*37*), *P. y. yoelii* NDH-II can oxidize deamino-NADH (K_m = 58 μM, V_{max} = 15 U/mg protein) and NADPH (K_m = 157 μM, V_{max} = 44 mU/mg protein) (Fig. 5A). V_{max}/K_m ratios indicate that *Plasmodium* NDH-II is more specific to NADH compared to NAD(P)H dehydrogenases from red beet root mitochondria [NDI (*38*) and NDE (*39*)].

Since mammalian hosts lack NDH-II, this enzyme is a promising target for new antiplasmodial agents. However, inhibitors for NDH-II are rare and mostly unspecific (*34*). Fry *et al.* (*11*) examined effects of inhibitors on ATP level in erythrocytic *P. falciparum* and found that 2-heptyl-4-hydroxyquinoline *N*-oxide (HQNO) and 5-hydroxy-2-methyl-1,4-naphthoquinone (plumbagin) showed antimalarial activities with IC_{50} values of 4.0 and 3.5 μM, respectively. In yeast, quinolone analogues HQNO and aurachin C 0-11 were shown to inhibit NDI1 with the IC_{50} values of 8 and 0.2 μM, respectively (*40*). In this study, we examined effects of HQNO and aurachin C 1-10 (*41*) on NADH:Q_1 reductase activity and determined IC_{50} values to be 2.5 and 0.5 μM, respectively (Fig. 5). Our data indicate that the quinolone analogues are potent inhibitors for *Plasmodium* NDH-II. Trifluoroperazine, the uncompetitive inhibitor in terms of Q_2 for *Mycobacterium tuberculosis* NDH-II (IC_{50} = 12 μM) (*42*), reduced the NADH:Q_1 reductase activity to 26% of the control at 100 μM.

DISCUSSION

Properties of Plasmodium Complex II—Parasitic nematodes adapted to hypoxic host environments, have modified respiratory chain, where isoforms of complex II serve as fumarate reductase (*43*, *44*). Kinetic properties of *P. y. yoelii* complex II are similar to those of mammalian enzymes and thus suitable for catalysing the